

INFORMATION TO USERS

This reproduction was made from a copy of a document sent to us for microfilming. While the most advanced technology has been used to photograph and reproduce this document, the quality of the reproduction is heavily dependent upon the quality of the material submitted.

The following explanation of techniques is provided to help clarify markings or notations which may appear on this reproduction.

1. The sign or "target" for pages apparently lacking from the document photographed is "Missing Page(s)". If it was possible to obtain the missing page(s) or section, they are spliced into the film along with adjacent pages. This may have necessitated cutting through an image and duplicating adjacent pages to assure complete continuity.
2. When an image on the film is obliterated with a round black mark, it is an indication of either blurred copy because of movement during exposure, duplicate copy, or copyrighted materials that should not have been filmed. For blurred pages, a good image of the page can be found in the adjacent frame. If copyrighted materials were deleted, a target note will appear listing the pages in the adjacent frame.
3. When a map, drawing or chart, etc., is part of the material being photographed, a definite method of "sectioning" the material has been followed. It is customary to begin filming at the upper left hand corner of a large sheet and to continue from left to right in equal sections with small overlaps. If necessary, sectioning is continued again—beginning below the first row and continuing on until complete.
4. For illustrations that cannot be satisfactorily reproduced by xerographic means, photographic prints can be purchased at additional cost and inserted into your xerographic copy. These prints are available upon request from the Dissertations Customer Services Department.
5. Some pages in any document may have indistinct print. In all cases the best available copy has been filmed.

**University
Microfilms
International**

300 N. Zeeb Road
Ann Arbor, MI 48106

8423111

Yeh, Taun-luan

IONIC EQUILIBRIA IN PYRIDINE-IODINE SOLUTIONS

City University of New York

PH.D. 1984

**University
Microfilms
International** 300 N. Zeeb Road, Ann Arbor, MI 48106

IONIC EQUILIBRIA IN PYRIDINE-IODINE SOLUTIONS

by

TAUN-IUAN YEH

A dissertation submitted to the Graduate Faculty
in Chemistry in partial fulfillment of the requirements
for the degree of Doctor of Philosophy,
The City University of New York

1984

This manuscript has been read and accepted for the Graduate Faculty in Chemistry in satisfaction of the dissertation requirement for the degree of Doctor of Philosophy.

2/24/84
date

Seymour Aronson
Chairman of Examining Committee

3/14/84
date

A. M. [Signature]
Executive Officer

[Signature]

[Signature]

[Signature]
Supervisory Committee

The City University of New York

ABSTRACT

IONIC EQUILIBRIA IN PYRIDINE-IODINE SOLUTIONS

by

TAUN-IUAN YEH

ADVISOR: PROFESSOR SEYMOUR ARONSON

A study was made of ionic equilibria in solutions of iodine and pyridine in n-heptane. A significant difference was found between freshly prepared and stored pyridine-iodine solutions. The experimental data for the stored solutions were reproducible and consistent.

EMF measurements were performed on cells of the type $Pt|I_2, KI(C1)in\ Py||I_2, KI(C2)in\ Py|Pt$. For the proposed dissociation of the molecular complex, the degree of ionization, the equilibrium constant and the enthalpy and entropy changes were calculated. Measurements of cyclic voltammetry, UV-Vis spectroscopy and Raman spectroscopy were also made.

Conductivity and concentration cell measurements have yielded more information about the reactions occurring in the system. It is anticipated that the results of this

research will increase our understanding of the formation and interaction of ionic species in organic systems and will extend the field of non-aqueous electrolytes.

Acknowledgments

I wish to thank my mentor, Professor Seymour Aronson, without whom this work would not exist. His technical guidance, patience and invaluable knowledge have made this report a reality. The thanks here cannot fully show my deep appreciation. No less important is my wife who encouraged and inspired my research.

I would like to thank my thesis committee, Professors Grace M. Wieder, Fitzgerald B. Bramwell and Jack Morrow for contributing their time and advice throughout the course of this research. Professor Wieder deserves special mention for contributing her extensive knowledge of Raman Spectroscopy.

It is a pleasure to acknowledge the skillful and timely glasswork of Mr. Ottmar Safferling who fabricated most of my glass equipment and made numerous quick repairs.

Finally ,my thanks and good wishes to all the friendly people who helped me in a variety of ways and who made my graduate years more pleasureable. I shall not attempt to list them here, but they will be long remembered.

Taun-Iuan Yeh

CONTENTS

ABSTRACT	iii
ACKNOWLEDGMENTS	v
<u>Chapter</u>	<u>page</u>
I. INTRODUCTION	1
II. EXPERIMENTAL	5
CHEMICALS	5
SPECTRAL MEASUREMENTS	8
VOLTAMMETRIC MEASUREMENTS	8
ELECTROCHEMICAL AND CONDUCTIVITY MEASUREMENTS	9
III. RESULTS AND DISCUSSION	13
ELECTROCHEMICAL MEASUREMENTS	13
Stability with time	15
Stored solutions measurements	16
Temperature dependence of the equilibrium constant	25
VOLTAMMETRIC MEASUREMENTS	31
Literature review	31
Comparison of reference electrodes	33
Iodide-Iodine Voltammetry in Acetonitrile	35
Iodide-Iodine Voltammetry in Pyridine	41
SPECTRAL MEASUREMENTS	46
Raman scattering measurements	47
UV-Vis absorption measurements	49
Absorption measurements in pure pyridine	50
Absorption measurements in mixtures of pyridine with n-heptane	55
CONDUCTIVITY AND I ₂ CONCENTRATION CELL MEASUREMENTS	60
Conductivity measurements	60
I ₂ concentration cell measurements	61
IV. OVERVIEW OF THE PYRIDINE-IODINE COMPLEXATION AND DISSOCIATION REACTIONS	70

<u>Appendix</u>	<u>page</u>
A. EMF DATA IN PURE PYRIDINE SOLUTIONS	76
B. EMF DATA IN PYRIDINE-HEPTANE SOLUTIONS	83
C. TEMPERATURE EFFECT ON THE EMF DATA	96
REFERENCES	102

LIST OF TABLES

<u>Table</u>	<u>page</u>
1. EMF data on the cell Pt I ₂ (0.315M),KI(C1,M) I ₂ (0.315M),KI(C2,M) Pt ^a	21
2. Summary of data from electrochemical cells of the type described by Line Diagram 8	23
3. Summary of data from electrochemical cells of the type describe by Line Diagram 16	24
4. Temperature effect on the EMF data on the cell Pt I ₂ (0.317M),NaI(C1,M) I ₂ (0.317M),NaI(C2,M) Pt ^a	27
5. Summary of the thermodynamic data in Py for the reaction 2PyI ₂ = Py ₂ I ⁺ + I ₃ ⁻	29
6. Temperature effect on the EMF data on the cell	30
7. Reference electrode comparisons	34
8. Polarographic Data for Iodide	37
9. Polarographic Data for Iodide-Iodine in the presence of 1.0M pyridine	40
10. Polarographic Data for Iodide-Iodine	44
11. Summary of data from conductivity cells	64
12. Summary of conductivity data on iodine dissolved in pyridine-heptane mixtures	65
13. EMF data on the cell Pt I ₂ (C1,M) in Py I ₂ (C2,M) in Py Pt ^a	68
14. EMF data on the cell Pt I ₂ (C1,M) in Py- Hep I ₂ (C2,M) in Py-Hep Pt ^e	69
15. Pyridine-iodine complexation reactions in pure pyridine	74

16.	Pyridine-iodine complexation reactions in Pyridine-Heptane mixtures	75
17.	EMF data on the cell $\text{Pt} \text{I}_2(0.0197\text{M}),\text{KI}(\text{C1},\text{M}) \text{I}_2(0.0197\text{M}),\text{KI}(\text{C2},\text{M}) \text{Pt}^{\text{a}}$	77
18.	EMF data on the cell $\text{Pt} \text{I}_2(0.0394\text{M}),\text{KI}(\text{C1},\text{M}) \text{I}_2(0.0394\text{M}),\text{KI}(\text{C2},\text{M}) \text{Pt}^{\text{a}}$	78
19.	EMF data on the cell $\text{Pt} \text{I}_2(0.0788\text{M}),\text{KI}(\text{C1},\text{M}) \text{I}_2(0.0788\text{M}),\text{KI}(\text{C2},\text{M}) \text{Pt}^{\text{a}}$	79
20.	EMF data on the cell $\text{Pt} \text{I}_2(0.1575\text{M}),\text{KI}(\text{C1},\text{M}) \text{I}_2(0.1575\text{M}),\text{KI}(\text{C2},\text{M}) \text{Pt}^{\text{a}}$	80
21.	EMF data on the cell $\text{Pt} \text{I}_2(0.629\text{M}),\text{KI}(\text{C1},\text{M}) \text{I}_2(0.629\text{M}),\text{KI}(\text{C2},\text{M}) \text{Pt}^{\text{a}}$	81
22.	EMF data on the cell $\text{Pt} \text{I}_2(1.257\text{M}),\text{KI}(\text{C1},\text{M}) \text{I}_2(1.257\text{M}),\text{KI}(\text{C2},\text{M}) \text{Pt}^{\text{a}}$	82
23.	EMF data on the cell $\text{Pt} \text{I}_2(0.0397\text{M}),\text{N}(\text{Bu})_4\text{I}(\text{C1},\text{M}) \text{I}_2(0.0397\text{M}),\text{N}(\text{Bu})_4\text{I}(\text{C2},\text{M}) \text{Pt}^{\text{a}}$	84
24.	EMF data on the cell $\text{Pt} \text{I}_2(0.0387\text{M}),\text{N}(\text{Bu})_4\text{I}(\text{C1},\text{M}) \text{I}_2(0.0387\text{M}),\text{N}(\text{Bu})_4\text{I}(\text{C2},\text{M}) \text{Pt}^{\text{a}}$	85
25.	EMF data on the cell $\text{Pt} \text{I}_2(0.0805\text{M}),\text{N}(\text{Bu})_4\text{I}(\text{C1},\text{M}) \text{I}_2(0.0805\text{M}),\text{N}(\text{Bu})_4\text{I}(\text{C2},\text{M}) \text{Pt}^{\text{a}}$	86
26.	EMF data on the cell $\text{Pt} \text{I}_2(0.0787\text{M}),\text{N}(\text{Bu})_4\text{I}(\text{C1},\text{M}) \text{I}_2(0.0787\text{M}),\text{N}(\text{Bu})_4\text{I}(\text{C2},\text{M}) \text{Pt}^{\text{a}}$	87
27.	EMF data on the cell $\text{Pt} \text{I}_2(0.152\text{M}),\text{N}(\text{Bu})_4\text{I}(\text{C1},\text{M}) \text{I}_2(0.152\text{M}),\text{N}(\text{Bu})_4\text{I}(\text{C2},\text{M}) \text{Pt}^{\text{a}}$	88
28.	EMF data on the cell $\text{Pt} \text{I}_2(0.158\text{M}),\text{N}(\text{Bu})_4\text{I}(\text{C1},\text{M}) \text{I}_2(0.158\text{M}),\text{N}(\text{Bu})_4\text{I}(\text{C2},\text{M}) \text{Pt}^{\text{a}}$	89
29.	EMF data on the cell $\text{Pt} \text{I}_2(0.311\text{M}),\text{N}(\text{Bu})_4\text{I}(\text{C1},\text{M}) \text{I}_2(0.311\text{M}),\text{N}(\text{Bu})_4\text{I}(\text{C2},\text{M}) \text{Pt}^{\text{a}}$	90

30.	EMF data on the cell	
	$\text{Pt} \text{I}_2(0.315\text{M}),\text{N}(\text{Bu})_4\text{I}(\text{C1},\text{M}) \text{I}_2(0.315\text{M}),\text{N}(\text{Bu})_4\text{I}(\text{C2},\text{M}) \text{Pt}^a$	91
31.	EMF data on the cell	
	$\text{Pt} \text{I}_2(0.633\text{M}),\text{N}(\text{Bu})_4\text{I}(\text{C1},\text{M}) \text{I}_2(0.633\text{M}),\text{N}(\text{Bu})_4\text{I}(\text{C2},\text{M}) \text{Pt}^a$	92
32.	EMF data on the cell	
	$\text{Pt} \text{I}_2(0.630\text{M}),\text{N}(\text{Bu})_4\text{I}(\text{C1},\text{M}) \text{I}_2(0.630\text{M}),\text{N}(\text{Bu})_4\text{I}(\text{C2},\text{M}) \text{Pt}^a$	93
33.	EMF data on the cell	
	$\text{Pt} \text{I}_2(1.257\text{M}),\text{N}(\text{Bu})_4\text{I}(\text{C1},\text{M}) \text{I}_2(1.257\text{M}),\text{N}(\text{Bu})_4\text{I}(\text{C2},\text{M}) \text{Pt}^a$	94
34.	EMF data on the cell	
	$\text{Pt} \text{I}_2(1.261\text{M}),\text{N}(\text{Bu})_4\text{I}(\text{C1},\text{M}) \text{I}_2(1.261\text{M}),\text{N}(\text{Bu})_4\text{I}(\text{C2},\text{M}) \text{Pt}^a$	95
35.	Temperature effect on the EMF data on the cell	
	$\text{Pt} \text{I}_2(0.0422\text{M}),\text{NaI}(\text{C1},\text{M}) \text{I}_2(0.0422\text{M}),\text{NaI}(\text{C2},\text{M}) \text{Pt}^a$	97
36.	Temperature effect on the EMF data on the cell	
	$\text{Pt} \text{I}_2(0.0778\text{M}),\text{NaI}(\text{C1},\text{M}) \text{I}_2(0.0778\text{M}),\text{NaI}(\text{C2},\text{M}) \text{Pt}^a$	98
37.	Temperature effect on the EMF data on the cell	
	$\text{Pt} \text{I}_2(0.157\text{M}),\text{NaI}(\text{C1},\text{M}) \text{I}_2(0.157\text{M}),\text{NaI}(\text{C2},\text{M}) \text{Pt}^a$	99
38.	Temperature effect on the EMF data on the cell	
	$\text{Pt} \text{I}_2(0.628\text{M}),\text{NaI}(\text{C1},\text{M}) \text{I}_2(0.628\text{M}),\text{NaI}(\text{C2},\text{M}) \text{Pt}^a$	100
39.	Temperature effect on the EMF data on the cell	
	$\text{Pt} \text{I}_2(1.265\text{M}),\text{NaI}(\text{C1},\text{M}) \text{I}_2(1.265\text{M}),\text{NaI}(\text{C2},\text{M}) \text{Pt}^a$	101

LIST OF FIGURES

<u>Figure</u>	<u>page</u>
1. Cell for voltammetry experiments:	11
2. Cell for electrochemical measurements	12
3. Variation of percentage ionization of PyI_2 with time in pure pyridine	19
4. Variation of percentage ionization of PyI_2 with	20
5. The upper curve gives the EMF data on a cell of the type	22
6. Variation of the equilibrium constant for 0.317M PyI_2 in pure pyridine with temperature	28
7. DC and diff. pulse polarography of 0.00105M I^-	36
8. DC and diff. pulse polarography of 0.00105M I^- ,	39
9. Cyclo-Voltammetry of 0.00103M iodide ion and	43
10. Cyclo-Voltammetry of 0.0802M iodine in pyridine	45
11. upper curve: Raman spectroscopy of 0.318M iodine, fresh (full line) and stored (broken line) in pure pyridine.	48
12. Variation of molar absorptivity of iodine at 367nm with time in pure pyridine.	51
13. upper curve: UV-Vis spectroscopy of 0.085M iodine, fresh (full line) and stored (broken line) in pure pyridine.	53
14. upper curve: UV-Vis spectroscopy of 0.0085M iodine, fresh (full line) and stored (broken line) in pure pyridine.	56
15. Variation of molar absorptivity of iodine at	57
16. UV-Vis spectroscopy of 0.00045M iodine, fresh	59

17. Variation of specific conductivity with iodine concentration and storage time for pure pyridine solutions. 66
18. Variation of specific conductivity with iodine concentration and storage time for pyridine-heptane mixtures. 67

Chapter I

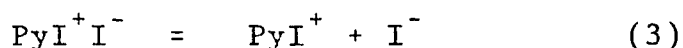
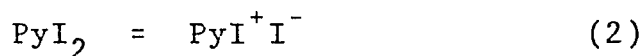
INTRODUCTION

Iodine reacts with pyridine in organic solvents to form a stable molecular complex¹⁻³. The chemical reaction for the complexation can be written



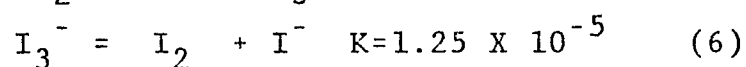
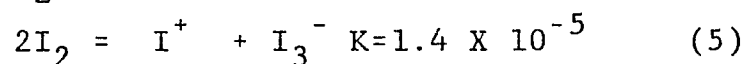
The equilibrium constant at room temperature is in the range of 2×10^2 l/mole^{3,4} and the heat of complexation is about -8 Kcal/mole^{2,4}.

Iodine dissolves in pyridine to form an electrolytic solution with electric conductivity comparable to aqueous salt solution. Several investigators have tried to elucidate the nature of these ionic solutions^{1,3,5-9}. Mulliken³ suggested a reaction sequence for the ionization of PyI_2 as follows:



Equations 2 and 3 show first the formation of an ion pair and then the dissociation into solvent-separated ions. Reid and Mulliken³ were unable to elucidate the nature of the ionic complex through a spectrophotometric study of dilute solutions, with I_2 in the range of 10^{-4} to 10^{-6} M.

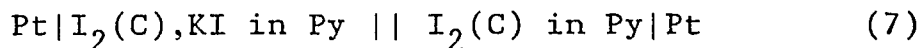
The behavior of halogens and halogen complexes in pyridine has recently been reviewed by Nigretto and Jozefowicz⁹. These same investigators performed a voltammetric analysis of pyridine-iodine solutions in a series of pH buffers⁸ with I₂ concentrations in the range of 10⁻³. They deduced apparent disproportionation constants, K, for the following equilibria:



Their disproportionation constant for Eq. 4 is in good agreement with a value calculated from voltammetric analysis of iodine solutions in acetonitrile in the presence of pyridine⁷ but is in poor agreement with a value obtained from conductivity measurements⁵.

With the exception of the above-mentioned studies, little quantitative information is available on ionic equilibria in pyridine-iodine solutions. The reliability of data obtained in these solutions has been questioned because slow, spontaneous changes in solution properties have been observed especially in very dilute solutions^{1,5,9}.

In a recent investigation, Aronson et al¹¹ have employed electrochemical cell measurements to obtain information on ionic equilibria in fresh pyridine-iodine solutions with high I₂ concentrations ranging from 0.16M to 1.58M. Their electrochemical cells were of the type



where C represents the nominal concentration of elemental iodine in pyridine. They applied a simple mechanism for the ionization of pyridine-iodine molecular complex system which was previously proposed^{1,3,8,9}.



The chemical symbols do not necessarily represent actual molecular species. In particular, I_2 on the left in Reaction 5 is most likely the molecular complex PyI_2 . The positive ion, I^+ , may be in the form Py_2I^+ or PyI^+ with the former more likely in pure pyridine. The results indicate that 8-18% ionization of the pyridine-iodine occurs. The values for the equilibrium constant for the ionization of pyridine-iodine complex corresponding to Reaction 5 range from 2×10^{-3} to 1×10^{-2} . This large variation in equilibrium constant indicates that their proposed mechanism may require modification.

In this investigation, we employed the same type of electrochemical cell measurements. The range of iodine concentrations has been expanded ten times more than that of Aronson et al¹¹. We also find a significant difference between fresh and stored pyridine-iodine solutions. For the stored pyridine-iodine solutions, the experimental data are reproducible and consistent. The results indicate that about 24% ionization of the pyridine-iodine complex occurs and the value of the equilibrium constant for Reaction 5 is fairly

constant, 2.4×10^{-2} . In a complementary study of iodine in pyridine-heptane solvent mixtures, with up to 30% heptane, the same values for percentage ionization and equilibrium constant were found as for pure pyridine. The dielectric constant of the solutions ranged from 12.35 to 9.22. Studies of cyclic voltammetry, UV-visible and Raman Spectroscopy, conductivity and iodine concentration cell measurements yielded additional information about the reactions occurring in the pyridine-iodine solutions.

Chapter II

EXPERIMENTAL

2.1 CHEMICALS

Materials were prepared and purified as follows:

Fisher certified ACS grade pyridine was allowed to stand over solid potassium hydroxide for several days, then refluxed over calcium hydride for several hours and repeatedly distilled from fresh portions of this hydride with a B.P. 115-115.5°C at 760mm. The first and final fractions were always rejected. This procedure sufficed to give a highly purified and anhydrous pyridine whose specific conductivity was below $10^{-7}(\text{ohm-cm})^{-1}$.

Iodine (Fisher ACS grade) was resublimed twice and kept in a desiccator over calcium sulfate before use.

Fisher certified HPLC grade n-heptane was dried and distilled over calcium hydride. A middle fraction was collected. A 20% solution of n-heptane in pyridine showed a specific conductance of $5 \times 10^{-7}(\text{ohm-cm})^{-1}$.

Fisher certified HPLC grade acetonitrile was dried over calcium hydride and refluxed over phosphorous(V) oxide for

several hours and repeatedly distilled from fresh portions of this oxide. A middle fraction was retained.

Potassium iodide, sodium iodide(Fisher ACS grade) and tetra-butylammonium iodide(Alfa products) were dried and stored in a vacuum desiccator before use. Picric acid, tetra-butyl ammonium fluoroborate, tetra-ethyl ammonium bromide(Fisher ACS grade), silver nitrate(Baker analyzed reagent) and iodine(I) chloride (Alfa products) were used as received.

Tetra-ethyl ammonium picrate ,used as supporting electrolyte, was obtained by the metathesis of equimolar quantities of picric acid, HPi, and tetra-ethyl ammonium bromide , $(C_2H_5)_4NBr$. A solution of $(C_2H_5)_4NBr$ in water was added to a solution of HPi in hot methanol. The orange precipitate, $(C_2 H_5)_4N Pi$, was recrystallized twice from 95% ethanol. The product, dried at $110^{\circ}C$ and stored in a vacuum desiccator over phosphorous(V) oxide,had a m.p. of $255.6^{\circ}C$ (lit.,mp $255.5-255.8^{\circ}C^{12}$).

Monopyridineiodine(I) chloride was prepared from equimolar quantities of pyridine and iodine(I) chloride. A solution of iodine(I) chloride in carbon tetrachloride is slowly added,dropwise with constant swirling,to a solution of pyridine in carbon tetrachloride. The resulting yellow precipitate is collected by suction filtration, washed with several small portions of carbon tetrachloride, and air-

dried. The bright yellow needles, PyICl , were recrystallized twice from 95% ethanol. The final product dried in vacuum over phosphorous(V) oxide for 48 hours had a m.p. of 134.5°C (lit., mp $134-135^{\circ}\text{C}^{13}$).

Dipyridineiodine(I) nitrate-First, Dipyridinesilver(I) nitrate is prepared by dissolving dried, powdered silver nitrate in pure dry pyridine at a molar ratio of 1 to 2. The complex separates as a colorless crystalline solid on cooling. Second, a solution of equimolar quantities of iodine in chloroform is slowly added, dropwise with constant swirling, to a solution of Dipyridinesilver(I) nitrate in chloroform over a dry Ice-acetone bath, to just above the freezing temperatures. The addition of iodine is continued until a permanent orange-brown coloration of halogen is observed, which indicates that the reaction is complete. The silver iodide precipitate is removed by moisture-free filtration. The clear filtrate is poured slowly, with shaking, into dry ethyl ether cooled in a dry Ice-acetone bath. The precipitate which separates is filtered in a dry atmosphere and washed with cold dry ether until colorless. The final product dried in vacuum over phosphorous(V) oxide for 72 hours had a m.p. of $132-137^{\circ}\text{C}$ (lit., m.p. 137°C^{14}).

2.2 SPECTRAL MEASUREMENTS

UV-Vis absorption measurements were made in a Cary 17 spectrophotometer using clear quartz cells of thicknesses 10, 2 and 0.1mm (NSG precision cells Inc.). Raman scattering measurements were made in a Varian Cary 83 spectrophotometer (Model 75 Ion Laser as power supply), using a fire-flattened end of capillary tube (i.d. 1mm, 18mm long) as a liquid cell. The wavelength scale of the instrument was calibrated by using a standard indene solution.

2.3 VOLTAMMETRIC MEASUREMENTS

Cyclic voltammetric measurements were made using an EG&G Polarographic Analyzer (Model 174A), an MFE plotmatic 715 X-Y recorder and a rotating platinum disk working electrode (RPDE) connected to a Model IBM EC/219 controller. The counter electrode was a piece of platinum foil attached to platinum wire. All potential measurements refer to a reference electrode of silver (Leeds & Northrup Model 117226) and 0.1M silver nitrate in pyridine solution. A suitable cell design is shown in Figure 1. The cell consisted of three compartments separated by two fine-frit disks. A pyridine solution of 0.1M tetra-butyl ammonium fluoroborate was placed in the middle and working compartments as a supporting electrolyte. Before each experiment the RPDE was lightly polished with 0.05µm alumina paste.

2.4 ELECTROCHEMICAL AND CONDUCTIVITY MEASUREMENTS

The electrochemical measurements were made in 3-compartment cells in which separation of the three compartments was effected by two fine-frit disks. A pyridine-iodine solution of $(C_2H_5)_4NPI$ (tetra-ethyl ammonium picrate) was placed in the middle compartment as a salt bridge. All compartments were filled to the same level. Pieces of platinum foil attached to platinum wire leads were inserted into the end compartments and served as electrodes. Voltage measurement were made with a KEITHLEY Model 160B digital multimeter. The cell design is shown in Figure 2. All electrochemical measurements were made in a constant temperature water bath regulated to $25.0 \pm 0.1^\circ C$. All stored solutions were kept in a dry box filled with nitrogen gas.

Conductivity measurements were made using a standard conductivity cell with platinum electrodes and a YSI model 31 conductivity bridge. The cell constant was determined to be 0.1 cm^{-1} using a 0.10M solution of NaCl at $25.0^\circ C$.

The platinum electrodes and cells were cleaned by immersion in hot concentrated nitric acid and then in cleaning solution for several days, repeatedly rinsing with distilled water and further standing in distilled water for several days.

All solutions of iodine and pyridine or pyridine-heptane mixtures were prepared just before the first measurement of a property and that property was then measured at selected time intervals up to a total time of one month.

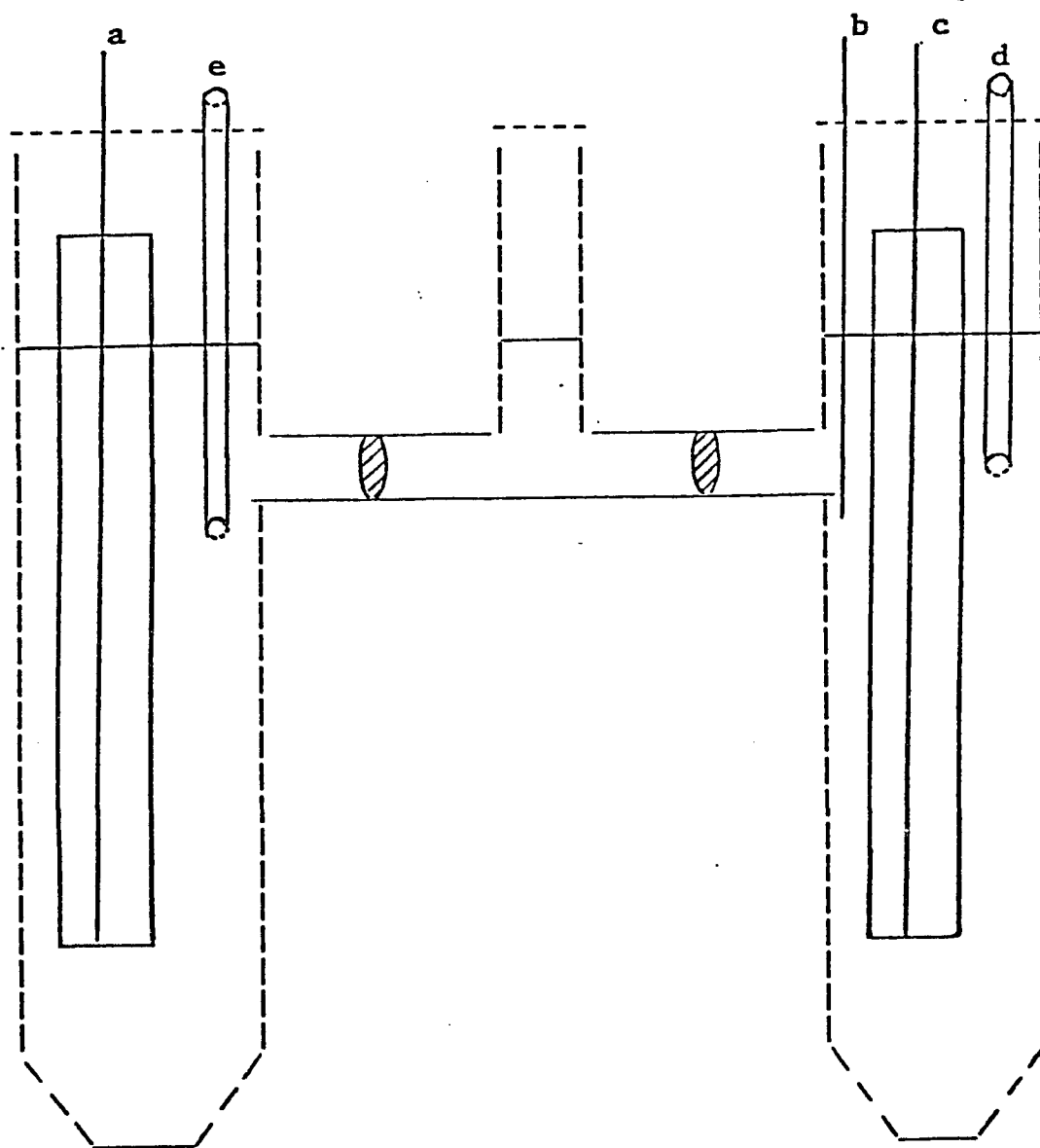


Figure 1: Cell for voltammetry experiments:
a. Reference electrode; Ag/AgNO_3 .
b. Auxiliary electrode; Pt wire.
c. Working electrode; Rotating Pt disk.
d. & e. bubble tubes for N_2 gas.

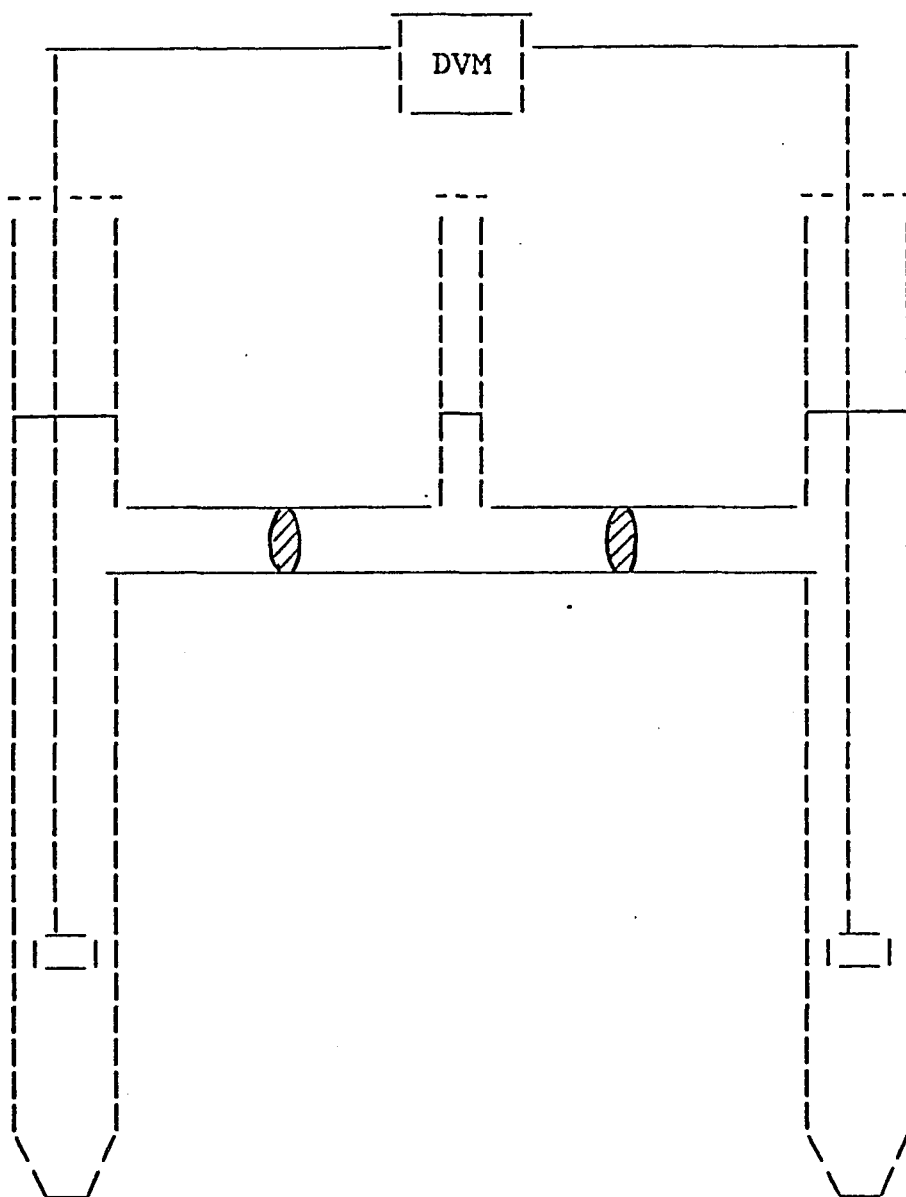


Figure 2: Cell for electrochemical measurements

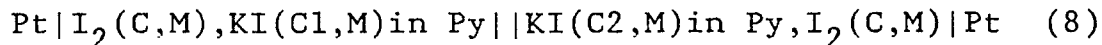
Chapter III

RESULTS AND DISCUSSION

In this section both experimental and calculated results will be presented. Appendix A,B and C list the experimental data and calculated activity of electro-species for each concentration of iodine in pure pyridine and in the mixtures of pyridine and n-heptane.

3.1 ELECTROCHEMICAL MEASUREMENTS

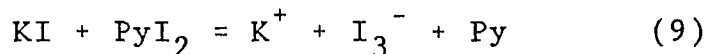
In my treatment of data from electrochemical cells of the type



where C represents the nominal concentration of elemental iodine in pyridine and C1 and C2 the nominal concentrations of added KI. We assume that the reaction



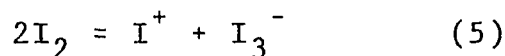
goes to completion. The equilibrium constant at room temperature is in the range of $2.0 \times 10^2 \text{ l/mole}$. We further assume that the reaction



goes to completion. Both of these assumption seem reasonable on the basis of the information available in the literature on the equilibrium constants for the formation of the

complex^{9,10} and the dissociation of KI in pyridine⁹. Since NaI and N(Bu)₄I have slightly greater dissociation constants, 3.7×10^{-4} and 4.1×10^{-4} , than KI, 2.1×10^{-4} , in pyridine, we will use these salts for the other electrochemical cells measurements.

We will obtain information on the equilibrium reaction in pyridine



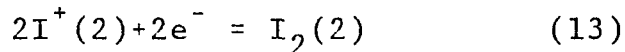
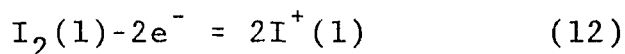
An equilibrium expression for Reaction 5 is

$$K = (a_{I^+})(a_{I_3^-}) / (a_{I_2})^2 \quad (10)$$

If the concentration of I₂ is kept approximately constant, than

$$KI = K(a_{I_2})^2 = (a_{I^+})(a_{I_3^-}) \quad (11)$$

Virtual electrochemical half-cell reactions for cells of the type described by Line Diagram 8 can be written as follows:



Where Half-cell 1 has KI(C1) and Half-cell 2 has KI(C2). For convenience, C1 is always greater than C2. The concentration of I₂ is assumed to be the same in both half-cells. The EMF in volts of such a cell at room temperature can be written as

$$E = -0.0591 \times \text{Log } a_{I^+}(1) / a_{I^+}(2) \quad (14)$$

We designate the equilibrium activity of I⁺ by the symbol Y1 when KI(C1) is present, by the symbol Y2 when KI(C2) is present and by the symbol X when no KI is present. We

assume nominal concentration C_1 and C_2 can be substituted for activity in the equilibrium expression. Assuming the dissociation in Reaction 5 to be small, we can write

$$K_1 = Y_1(Y_1+C_1) = Y_2(Y_2+C_2) = X^2 \quad (15)$$

We can solve for X, Y_1, Y_2 and K_1 using Equations 14 and 15.

3.1.1 Stability with time

Measurements were made in pyridine-iodine solutions at selected time intervals up to a total time of one month at 25°C on electrochemical cells of the type described by Line Diagram 8 with the same concentration of I_2 in both half-cells and KI present in both half-cells but at different concentrations. Measurements were always made using the three compartment cell with 0.3M $(C_2H_5)_4N^+Pi^-$ in the middle compartment. The nominal concentrations of iodine were 0.315M and 0.0785M.

In a preliminary investigation, we found the percentage ionization of PyI_2 in pyridine first increased with time, then levelled off at about 25% after 5 days. This is shown in Figure 3. The same treatment as above for iodine in a mixture of pyridine and n-heptane gave the results shown in Figure 4 which is in agreement with those in Figure 3. Further discussion will be given in the next section.

3.1.2 Stored solutions measurements

Based on the preliminary results in Figure 3, all measurements were made 5-10 days after solution preparation. The range of iodine concentration was from $1.97 \times 10^{-2} \text{M}$ to 1.261M.

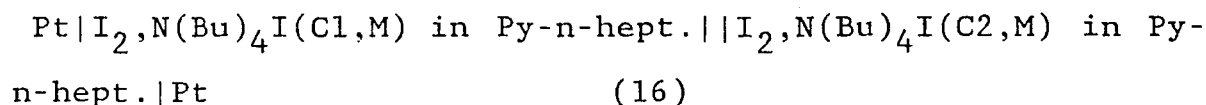
Data obtained on a cell of the type in Line Diagram 8 are presented in Table 1 and Figure 5. The nominal iodine concentration in both half cells was 0.315M and nominal KI or NaI concentrations used in an experiment ranged from 1.5% to 9.0% of the nominal iodine concentrations. After addition of the first aliquot of KI, the EMF value was measured intermittently over a period of 1 hour and was found to have a steady value of $1.73 \pm 0.02 \text{mv}$. The nominal KI or NaI concentration was then increased four additional times and EMF measurements were made. The calculated K_I and X were constant within experimental error. Data obtained at different iodine concentrations are given in Appendix A (Tables 17 to 22). All the experimental data were reproducible and consistent.

Data were obtained on cells with iodine concentrations ranging from 0.0197M to 1.261M. The nominal KI or NaI concentrations used in an experiment were from 1.5% to 9.0% of the nominal iodine concentrations. The calculated activities of I^+ and the percentage ionization of iodine on the basis of Reaction 5 are presented in Table 2. We use

both KI and NaI in our cells. The value for percentage ionization of pyridine-iodine complex in pure pyridine is fairly constant, 24.0 ± 0.7 , except for 0.0197M iodine.

Values for the equilibrium constant for the ionization of iodine in pyridine corresponding to Reaction 5 and Equation 10 were calculated from the data in Table 2. The value is fairly constant, 0.024 ± 0.003 , from 0.0394M I_2 to 1.261M I_2 . The deviation of 0.0197M I_2 may be a result of the complexity of the ionization of $Py-I_2$ in dilute solutions^{1,5,9}.

The same treatment as above can be used in mixtures of pyridine with n-heptane of varied dielectric constant. Measurements were made at 25°C on electrochemical cells of the type



These measurements should quantitatively relate the extent of ionic dissociation of the pyridine-iodine molecular complex to the dielectric constant and to the nature of the solvent system. The dielectric constant was varied from 12.35 (pure pyridine) to 9.22 (70% pyridine). The dielectric constants of the mixed solvents were calculated by use of the principle of additivity (i.e., $D_{cal} = X_{py} D_{py} + X_{hep} D_{hep}$).

Data obtained on cells with the same nominal iodine concentrations containing different nominal concentrations

of $N(\text{Bu})_4\text{I}$ in both half-cells are given in Appendix B (Tables 23 to 34). The summary data for the activities of I^+ and percentage ionization of iodine in mixtures of pyridine with n-heptane are presented in Table 3. The percentage ionization of the complex in the pyridine-heptane mixtures is the same, within experimental error, as in pure pyridine.

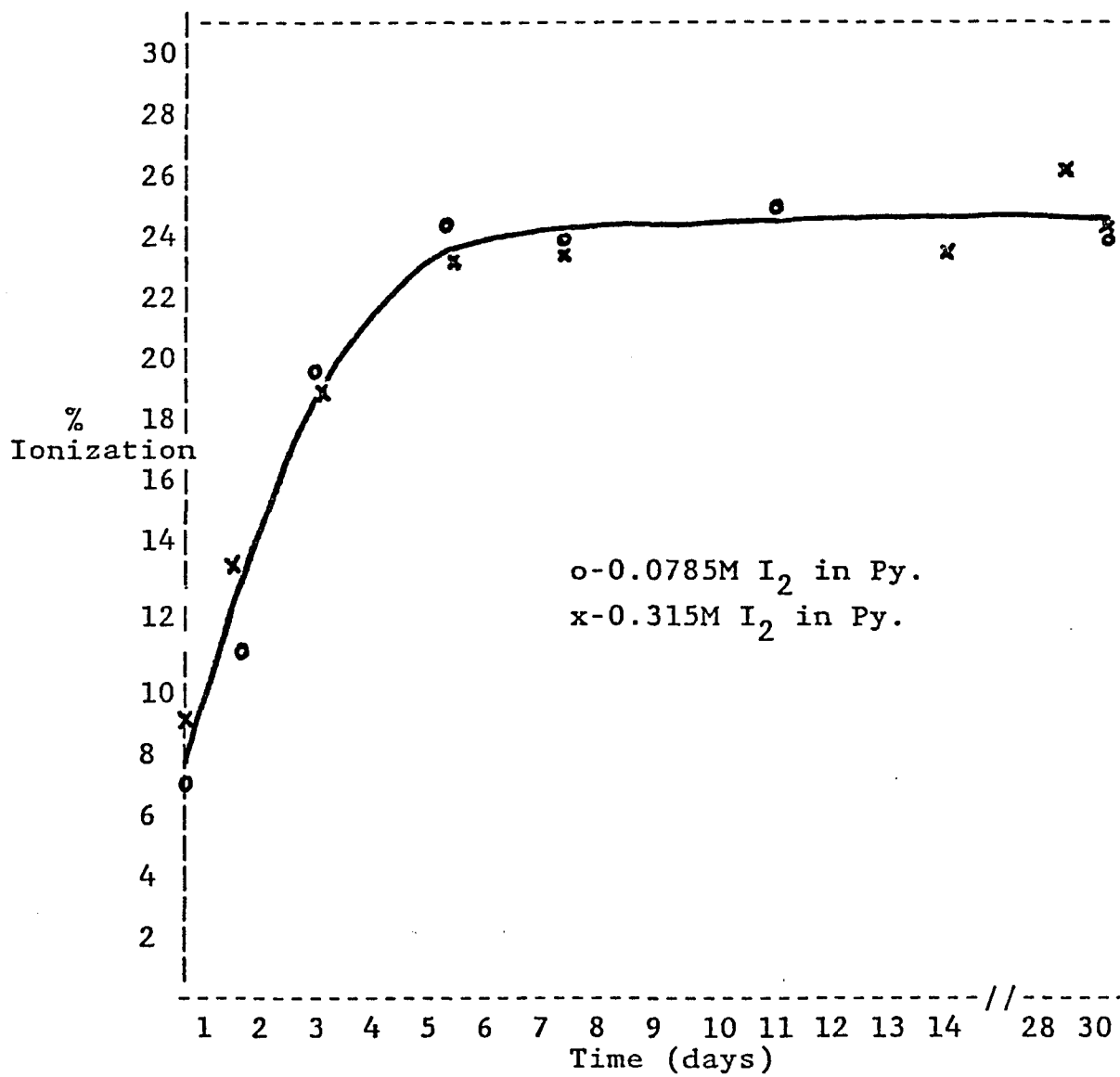


Figure 3: Variation of percentage ionization of PyI_2 with time in pure pyridine

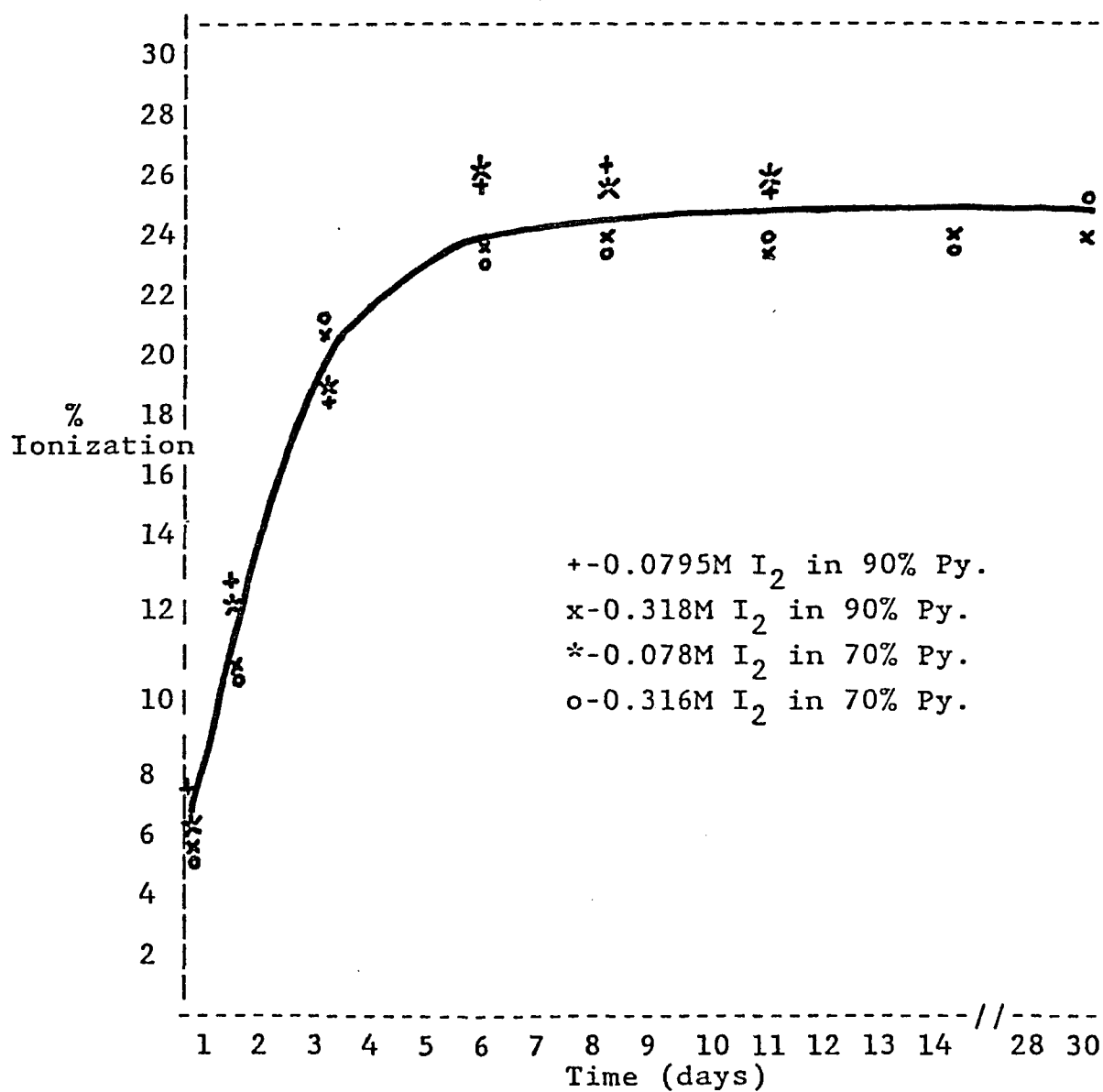


Figure 4: Variation of percentage ionization of PyI₂ with time in mixtures of pyridine and n-heptane.

TABLE 1

EMF data on the cell
 $\text{Pt} | \text{I}_2(0.315\text{M}), \text{KI}(C1, \text{M}) || \text{I}_2(0.315\text{M}), \text{KI}(C2, \text{M}) | \text{Pt}^{\text{a}}$

C1,M	C2,M	E,mv	Y1,M	Y2,M	K1,M ²	X,M
0.0102	0.00510	1.73	0.0328	0.0363	0.00141	0.0376
0.0148	0.00492	3.35	0.0306	0.0349	0.00139	0.0373
0.0189	0.00473	4.85	0.0287	0.0347	0.00137	0.0370
0.0228	0.00456	6.15	0.0276	0.0351	0.00139	0.0373
0.0264	0.00439	7.22	0.0271	0.0359	0.00145	0.0381

						0.0375 _± 0.0004

0.0112	0.00561	2.02	0.0300	0.0325	0.00124	0.0352
0.0162	0.00538	3.87	0.0282	0.0328	0.00125	0.0354
0.0207	0.00518	5.53	0.0264	0.0328	0.00125	0.0353
0.0249	0.00499	7.03	0.0251	0.0330	0.00125	0.0354
0.0288	0.00481	8.41	0.0238	0.0331	0.00125	0.0354

						0.0353 ^b _± 0.0001

a. In pure pyridine.

b. In this cell, the concentration of I_2 was 0.310M
 and NaI, rather than KI, was present in both half-cells.

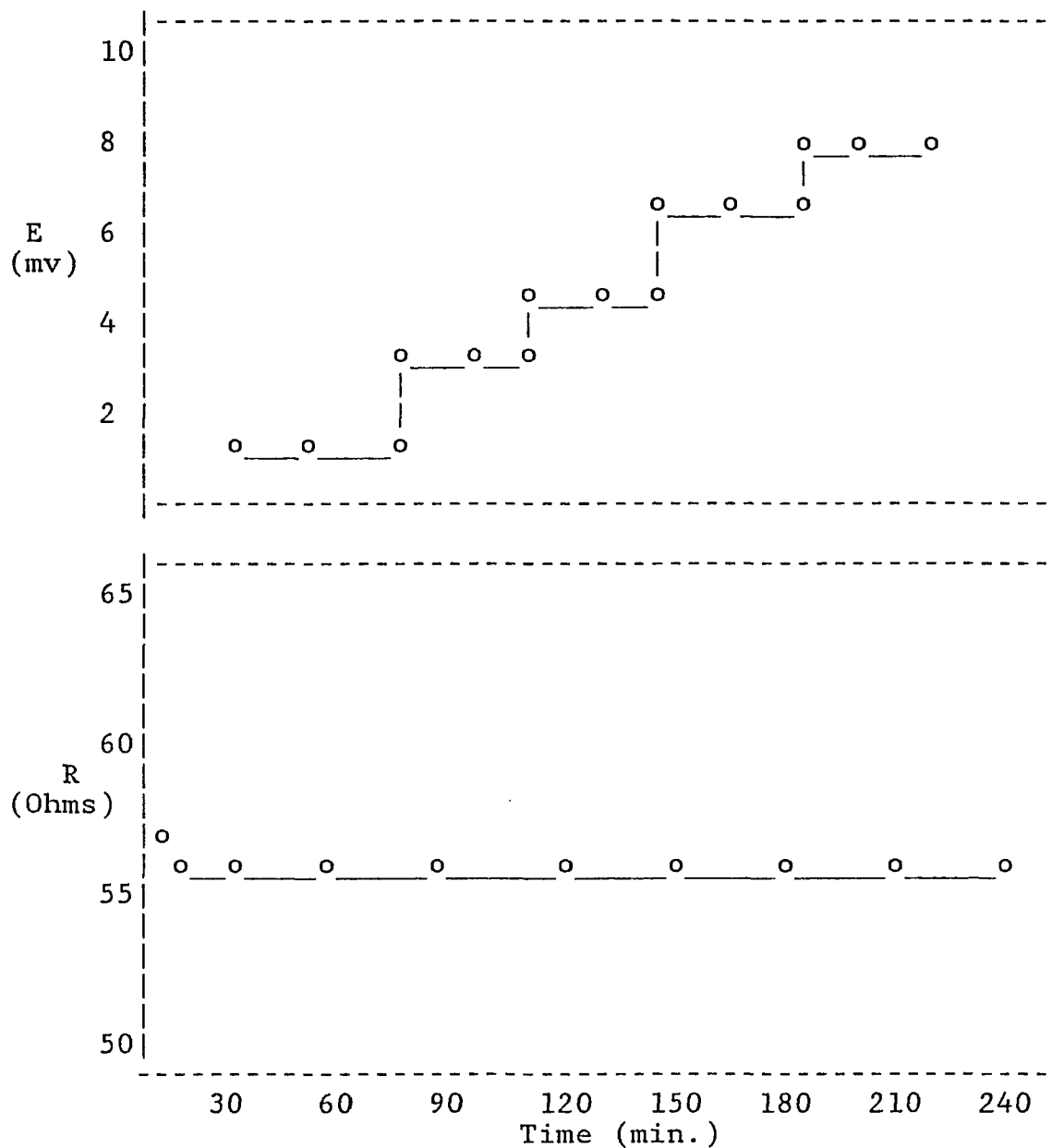


Figure 5: The upper curve gives the EMF data on a cell of the type
 $\text{Pt}|\text{I}_2(0.315\text{M}),\text{KI}(\text{C1},\text{M})||\text{I}_2(0.315\text{M}),\text{KI}(\text{C2},\text{M})|\text{Pt}.$
 The vertical dashed lines refer to additions of KI.
 The lower curve is the electrical resistance of 0.315M iodine in pyridine.

TABLE 2

Summary of data from electrochemical cells of the type
described by Line Diagram 8

I_2 , nominal Concn, M	I^+ , Activity, M	I_2 , Ionization, %
0.0197	0.0017 \pm 0.0006	17.2
0.0197 ^a	0.0018 \pm 0.0009	18.3
0.0394	0.0047 \pm 0.0001	23.8
0.0411 ^a	0.0052 \pm 0.0001	25.3
0.0788	0.0096 \pm 0.0008	24.3
0.0772 ^a	0.0097 \pm 0.0002	25.1
0.1575	0.0186 \pm 0.0003	23.6
0.1574 ^a	0.0179 \pm 0.0001	22.7
0.315	0.0375 \pm 0.0004	23.8
0.310 ^a	0.0353 \pm 0.0001	22.8
0.629	0.0762 \pm 0.0026	24.2
0.628 ^a	0.0745 \pm 0.0004	23.8
1.257	0.154 \pm 0.001	24.4
1.261 ^a	0.152 \pm 0.006	24.1
		24.0 \pm 0.7

a. NaI present in both half-cells.

TABLE 3

Summary of data from electrochemical cells of the type describe by Line Diagram 16

I_2 , nominal Concn, M	I^+ , Activity, M	I_2 , Ionization, %
0.0397 ^a	0.0049 \pm 0.0002	24.7
0.0407 ^b	0.0051 \pm 0.0002	25.1
0.0387 ^c	0.0048 \pm 0.0002	24.8
0.0378 ^d	0.0047 \pm 0.0002	24.9
0.0805 ^a	0.0107 \pm 0.0002	26.6
0.0795 ^b	0.0102 \pm 0.0001	25.7
0.0787 ^c	0.0104 \pm 0.0002	26.4
0.0798 ^d	0.0100 \pm 0.0002	25.1
0.152 ^a	0.0183 \pm 0.0001	24.1
0.159 ^b	0.0187 \pm 0.0001	23.5
0.158 ^c	0.0192 \pm 0.0004	24.3
0.159 ^d	0.0195 \pm 0.0002	24.5
0.311 ^a	0.0349 \pm 0.0004	22.4
0.314 ^b	0.0383 \pm 0.0005	24.4
0.315 ^c	0.0392 \pm 0.0006	24.9
0.311 ^d	0.0347 \pm 0.0005	22.3
0.633 ^a	0.0665 \pm 0.0011	21.0
0.631 ^b	0.0692 \pm 0.0001	21.9
0.630 ^c	0.0732 \pm 0.0013	23.2
0.633 ^d	0.0756 \pm 0.0004	23.9
1.257 ^a	0.136 \pm 0.002	21.6
1.259 ^b	0.152 \pm 0.001	24.1
1.261 ^c	0.126 \pm 0.001	20.0
1.261 ^d	0.149 \pm 0.002	23.6
		23.9 \pm 1.6

a. In 95% Py. and 5% Hep. system. dielectric constant=11.83
b. In 90% Py. and 10% Hep. system. dielectric constant=11.31
c. In 80% Py. and 20% Hep. system. dielectric constant=10.26
d. In 70% Py. and 30% Hep. system. dielectric constant=9.22

3.1.3 Temperature dependence of the equilibrium constant

A study was made of the temperature dependence of the dissociation. Data obtained are presented in Table 4. The nominal iodine concentration in both half cells was 0.317M and different nominal NaI concentrations used in an experiment were from 5.1% to 7.9% of nominal iodine concentration. The EMF value was measured at increasing temperatures from 25°C to 55°C in a thermostatted water bath, then at decreasing temperatures to 25°C. The nominal NaI concentration was then increased and EMF measurements were made at increasing and decreasing temperature again. The EMF and K_{eq} values shown in Table 4 indicate that the data are reproducible and reversible. Data obtained for other iodine concentrations are given in Appendix C (Tables 35 to 39). All experimental data were consistent and reproducible.

According to the Clausius-Clapeyron equation:

$$\text{Log } K = -\Delta H^{\circ}/2.303RT + C \quad (17)$$

a plot of the equilibrium constant of Reaction 5 for 0.317M I_2 versus reciprocal absolute temperature is shown in Figure 6. From the value of the slope in Figure 6 we have calculated enthalpy and entropy changes on the basis of Reaction 5 using the free energy functions:

$$\Delta G^{\circ} = -RT \ln K_{eq} \quad \text{and} \quad \Delta G^{\circ} = \Delta H^{\circ} - T\Delta S^{\circ} \quad (18)$$

It is observed in Table 5 that K_{eq} decreases with increasing temperature. The average values of the enthalpy and entropy changes respectively are $-2.67 \pm 0.17 \text{Kcal}$ and $-16.4 \pm 0.5 \text{cal/}^\circ\text{K}$. The negative heat of dissociation seems somewhat surprising at first glance since one might expect ionic dissociation to be endothermic. However, this effect is probably offset by the exothermic nature of I_3^- . In water, for example, the standard heat of formation of I_3^- from I_2 and I^- is $-5.1 \text{Kcal/mole}^{15}$. The negative entropy change can probably be explained on the basis of the ordering of the polar pyridine solvent molecules in the vicinity of the positive and negative ions.

The same treatment as above can be used for mixtures of pyridine with n-heptane. We selected 0.313M I_2 in a mixture of 80% pyridine with 20% n-heptane. Data obtained are presented in Table 6. The values of K_{eq} in Table 6 are close to the average values in Table 5. All the thermodynamic data in mixtures of pyridine with n-heptane are similar to those obtained in pure pyridine.

TABLE 4

Temperature effect on the EMF data on the cell
 $\text{Pt} | \text{I}_2(0.317\text{M}), \text{NaI}(C1, \text{M}) || \text{I}_2(0.317\text{M}), \text{NaI}(C2, \text{M}) | \text{Pt}^{\text{a}}$

Temp., °K	C1, M	C2, M	E, mv	X, M	K_{eq}
298	0.0162	0.00541	3.73	0.0366	0.0225
313	-----	-----	4.23	0.0339	0.0185
328	-----	-----	4.73	0.0317	0.0156
313	-----	-----	4.25	0.0337	0.0182
298	-----	-----	3.72	0.0367	0.0226
298	0.0250	0.00501	6.75	0.0371	0.0233
313	-----	-----	7.70	0.0340	0.0186
328	-----	-----	8.55	0.0320	0.0160
313	-----	-----	7.68	0.0341	0.0188
298	-----	-----	6.76	0.0370	0.0232

a. In pure pyridine.

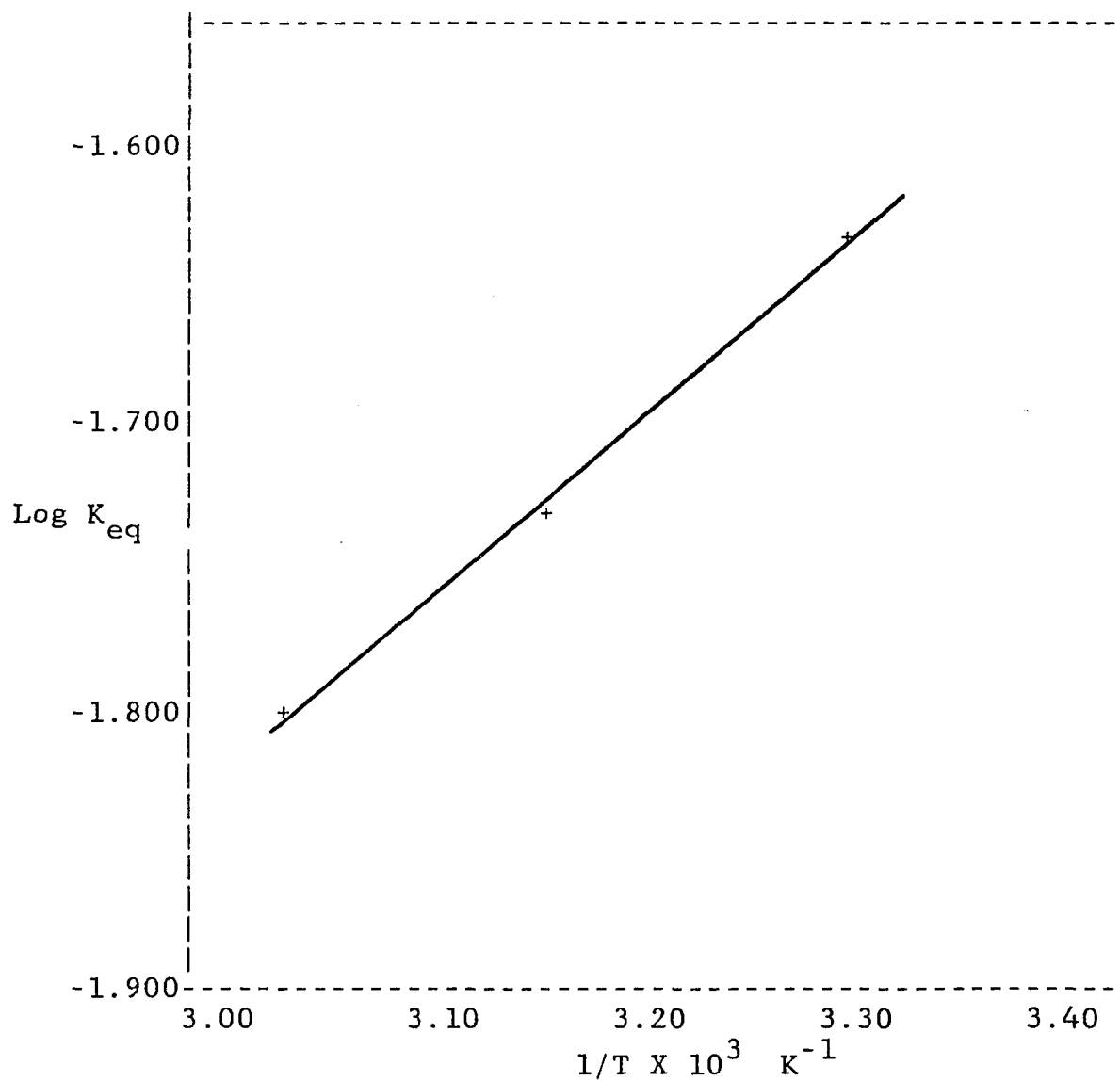
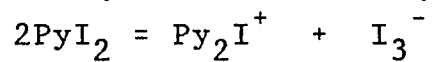


Figure 6: Variation of the equilibrium constant for 0.317M PyI_2 in pure pyridine with temperature

TABLE 5

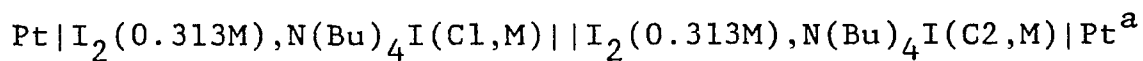
Summary of the thermodynamic data in Py for the reaction



$\text{I}_2, \text{Conc}, \text{M}$	K_{eq} at 25°C	$-\Delta H^\circ, \text{Kcal}$	$-\Delta S^\circ, \text{Cal}/^\circ\text{K}$
0.0422	0.0240	2.67	16.4
0.0778	0.0238	2.70	16.5
0.157	0.0227	2.64	16.4
0.317	0.0229	2.53	16.0
0.628	0.0237	2.48	15.8
1.265	0.0250	2.97	17.4
		----- 2.67±0.17	----- 16.4±0.5

TABLE 6

Temperature effect on the EMF data on the cell



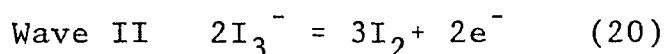
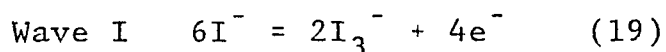
Temp., °K	C1,M	C2,M	E,mv	X,M	K _{eq}
298	0.0159	0.00531	3.62	0.0371	0.0241
313	-----	-----	4.10	0.0343	0.0197
328	-----	-----	4.57	0.0322	0.0168
313	-----	-----	4.12	0.0341	0.0194
298	-----	-----	3.64	0.0369	0.0237
298	0.0246	0.00492	6.68	0.0369	0.0237
313	-----	-----	7.59	0.0340	0.0192
328	-----	-----	8.38	0.0322	0.0168
313	-----	-----	7.61	0.0339	0.0191
298	-----	-----	6.65	0.0371	0.0241

a. In a mixture of 80% pyridine with 20% n-heptane.

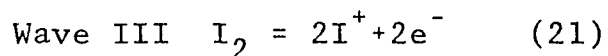
3.2 VOLTAMMETRIC MEASUREMENTS

3.2.1 Literature review

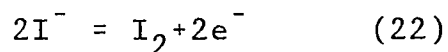
The voltammetric behaviour of the system $I^- - I_2 - I^+$ in different non-aqueous solvent has been extensively studied by several authors. The reactions of iodide in acetonitrile at a rotating platinum electrode were examined by Kolthoff and Coetzee¹⁸ and Popov and Geske¹⁹. Each produced polarograms showing two anodic steps attributed to reactions of the types given in Eqs. 19 and 20.



The first involves oxidation of iodide ion to triiodide ion and is a two-electron step. The second involves oxidation of triiodide ion to iodine and is a one-electron step. A two step oxidation of iodide to iodine was also observed by Nelson and Iwamoto²⁰ in nitromethane and acetone, by Plichon et al²¹ in acetic anhydride and by Guidelli and Piccardi²² in acetic acid. Dryhurst and Elving²³ observed that the electro-oxidation of iodide at a pyrolytic graphite electrode in acetonitrile solution gives three distinct anodic waves, involving Eqs. 19,20 and oxidation of iodine to unipositive iodine which is indicated in Eq. 21



Recently Pezzatini and Guidelli⁷ observed that the oxidation of iodide in the presence of pyridine in acetonitrile shows two steps consisting of (Wave I+Wave II) and Wave III. They observed that the first two partial waves tend to merge. This is qualitatively explained by complex formation between Py and I₂, which shifts the equilibrium $I_3^- = I_2 + I^-$ to the right. Iwamoto²⁴ also observed that electro-oxidation of iodide ion in pure pyridine was found to proceed via a two-step mechanism but of a different type. The electrode reactions are Eqs. 21 and 22.



Interestingly, the electro-oxidation of iodine in pyridine thus proceeds via a two-step process involving Wave II and Wave III. When a small amount of sodium iodide was added to the solution of iodine in pyridine, a three-step process involving Wave I, Wave II and Wave III was observed. It appears that the first step in electro-oxidation of iodine in pyridine involves oxidation of triiodide ion to iodine, followed by further oxidation of iodine to iodine(I) in the second step. This evidence supports our simple mechanism for the dissociation of iodine in pyridine in Reaction 5. In the next section, we obtained voltammetric data to find out if differences are observed between fresh and stored solutions.

3.2.2 Comparison of reference electrodes

It is often desirable to make comparisons of electrochemical potentials which have been measured under dissimilar conditions. In practice two situations are very often encountered, evaluation of potential measurements in different solvents, and evaluation of potential measurements in the same solvent with different reference electrodes. While evaluation of the effect of solvent variation involves formidable fundamental difficulties (e.g. uncertainty in the liquid junction potential), comparison of measurements made in one solvent but with different reference electrodes is often desirable and can be done if the relevant data are available. The common practice of using the aqueous SCE as an all-purpose reference electrode is convenient because it is otherwise necessary to provide a suitable reference electrode for each solvent used.

Based on our experimental conditions, we chose Ag/0.1M AgNO₃ and Ag/AgCl(s), LiCl(s) in a 0.1M N(Bu)₄BF₄ supporting electrolyte as our reference systems. Data for different reference electrodes are presented in Table 7.

We used two reference electrodes, Ag/AgNO₃ and Ag/AgCl, LiCl in our voltammetric measurements. Both electrodes gave us almost the same values of E_{1/2} for oxidation of the same species, to be discussed later, indicating that our values in Table 7 are reliable.

TABLE 7

Reference electrode comparisons

Solvent	Reference system	Temp.	E_{ref} vs SCE	Ref.
CH ₃ CN	Ag/0.1M AgNO ₃ / /0.1M N(Bu) ₄ BF ₄ /	25°C	0.320 ₋ 0.02	a
—	Ag/0.1M AgNO ₃ / /0.1M N(Et) ₄ ClO ₄ /	—	0.337	37
—	Ag/AgCl(s),LiCl(s)/	—	0.190	16
—	Ag/AgCl(s),LiCl(s)/ /0.1M N(Bu) ₄ BF ₄ /	—	-0.170 ₋ 0.05	a
Pyridine	Ag/0.1M AgNO ₃ / /0.1M N(Bu) ₄ BF ₄ /	—	0.037 ₋ 0.01	a
—	Ag/1.0M AgNO ₃	—	0.090	17

a. the present work.

3.2.3 Iodide-Iodine Voltammetry in Acetonitrile

The differential pulse and dc polarography of current-voltage curves of 0.00105M $N(Bu)_4I$ at a 2000 rpm rotating platinum disk at a scan rate of 10 mv/sec over the range of -0.2v to 1.5v in 0.1M $N(Bu)_4BF_4$ supporting electrolyte in acetonitrile show three anodic steps in Figure 7. Polarographic data for iodide ion are compared with previous investigators in Table 8. The first two waves in Figure 7 correspond to Eqs. 19 and 20. In support of the assigned reactions it was noted that, in each case, the first wave was twice the height of the second. That is in agreement with the stoichiometry of the reaction. Both Wave I and Wave II show fairly well formed anodic and cathodic waves, indicating that both waves are essentially reversible which is in agreement with the data of Popov and Geske¹⁹. Wave III corresponding to Eq. 21 appears to be completely irreversible. The upper curve in Figure 7 with the Ag/0.1M $AgNO_3$ reference electrode shows three anodic steps with $E_{1/2}$ values of about 0.375, 0.675 and 1.365 volt vs SCE, using the correction values in Table 7. The $E_{1/2}$ values obtained using Ag/AgCl(s), LiCl(s) as the reference electrode were 0.38, 0.67 and 1.28 volt vs SCE shows in the lower curve in Figure 7. The different reference systems gave almost the same results. Our data are compared to other investigators in Table 8. Our values for $E_{1/2}$ are very similar to those of Popov¹⁹ and Elving²³.

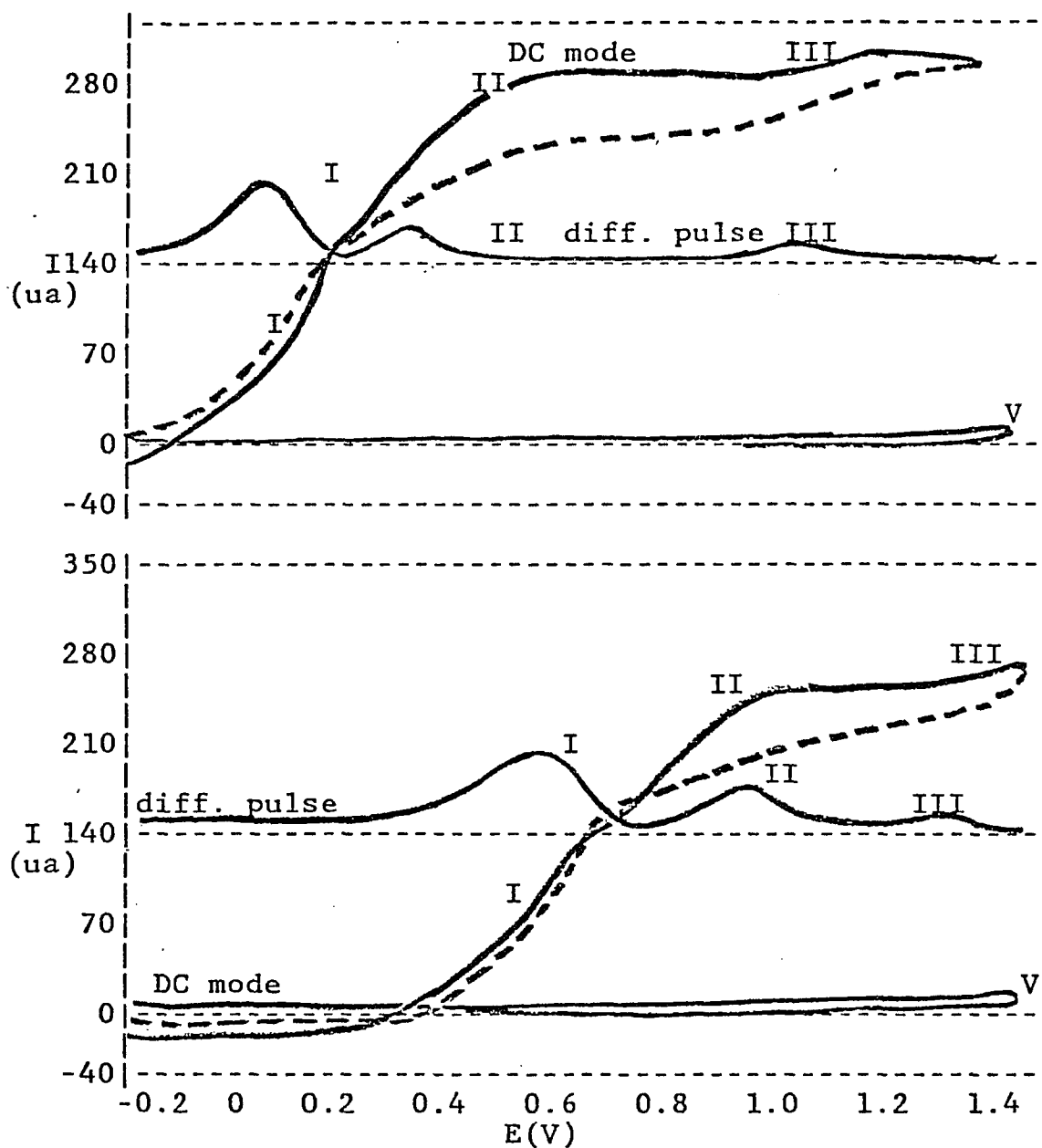


Figure 7: DC and diff. pulse polarography of 0.00105M I^- with different reference electrodes in acetonitrile.

The upper curve for $\text{Ag}/0.1\text{M AgNO}_3$.

The lower curve for $\text{Ag}/\text{AgCl(s)}, \text{LiCl(s)}$.

Wave I: Iodide = Triiodide.

Wave II: Triiodide = Iodine.

Wave III: Iodine = Iodine(I). V: Residual curve.

TABLE 8
Polarographic Data for Iodide

Compound	Solvent	Reference system	Temp. °C	$E_{1/2}$ (V)	Working electrode	Ref.
NaI	MeCN	SCE	25	0.3, 0.6	Pt	18
		/0.1M TEAP/				
NaI	MeCN	Ag/0.01M AgNO ₃ / /0.1M LiClO ₄ /	—	0.04, 0.37 1.15	Pt	19
I ⁻	MeCN	SCE	—	0.25, 0.55	Pt	24
		/0.1M NaClO ₄ /				
I ⁻	MeCN	Ag/0.1M AgNO ₃ / /0.1M TBAFB/	—	0.055, 0.355 1.045	Pt	a
—	—	Ag/AgCl, LiCl/ /0.1M TBAFB/	—	0.55, 0.84 1.35	Pt	a
I ⁻	MeCN	Ag/0.1M AgNO ₃ / /0.1M TEAP/	—	0.02, 0.37 1.00	PGE	23

a. the present work.

TEAP-Tetraethylammonium perchlorate.

PGE-Pyrolytic graphite Electrode.

TBAFB-Tetrabutylammonium Fluoroborate.

An approximately equimolar solution of iodide and iodine in the presence of 1.0M pyridine in acetonitrile show two anodic steps and one cathodic step in Figure 8. Both Wave I and Wave II in the upper and lower curves tend to merge to the same value of $E_{1/2}=0.605\text{v}$ vs SCE. There is a shift of $E_{1/2}$ in Wave III to the same value of 1.0v vs SCE for both reference electrodes. A cathodic step, corresponding to the reverse of Wave I, namely Wave II, corresponds to the reduction of triiodide ion to the iodide ion with $E_{1/2}$ for the upper and lower curves equal to the same value, 0.13v vs SCE. The polarographic data are given in Table 9. Our data show the same decreasing trend as Popov¹⁹ for Wave I, II and III, but are quite different from those of Elving²³ who used a stationary working electrode made from pyrolytic graphite. Interestingly, the height of positive iodine(I) in Wave III has increased tremendously as compared with Wave III in Figure 7. Wave III in Figure 8 can be regarded as a partially well-defined, quasireversible reaction. All the data shown in Tables 8 and 9 have indicated that pyridine increases the stability of positive iodine(I). All the $E_{1/2}$ values are lowered, indicating a decrease in the energy of the electro-active species in the system.

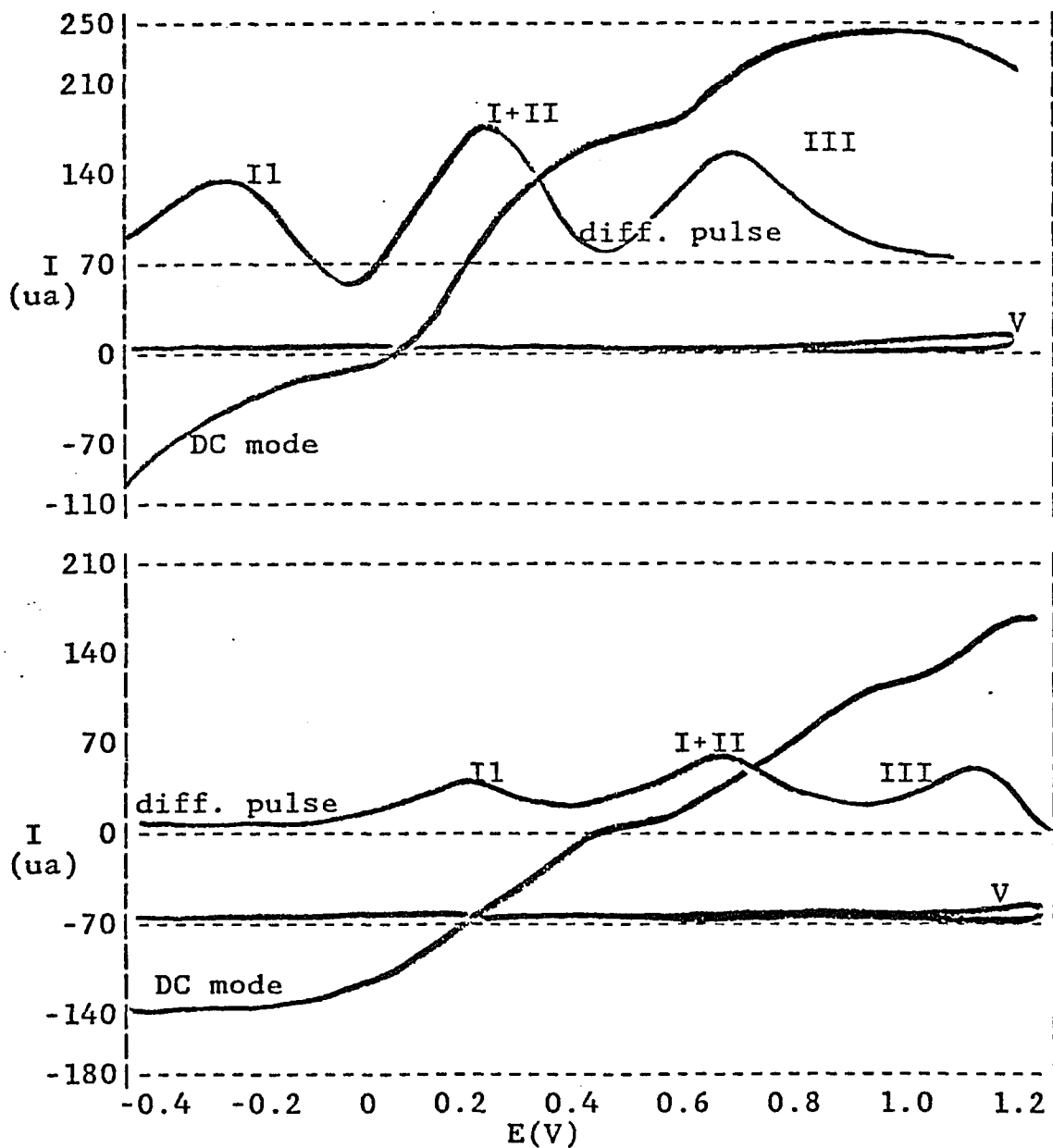


Figure 8: DC and diff. pulse polarography of 0.00105M I^- , 1.0M Py and 0.001M I_2 with different references electrode in acetonitrile.

The upper curve for $\text{Ag}/0.1\text{M AgNO}_3$.

The lower curve for $\text{Ag}/\text{AgCl}(\text{s}), \text{LiCl}(\text{s})$.

Wave II: Triiodide = Iodide.

Wave I+II: Triiodide + Iodide = Iodine.

Wave III: Iodine = Iodine(I). V: Residual curve.

TABLE 9

Polarographic Data for Iodide-Iodine in the presence of 1.0M pyridine

Compound	Solvent	Reference system	Temp. °C	$E_{1/2}$ (V)	Working electrode	Ref.
NaI/ I ₂ /	MeCN	Ag/0.01M AgNO ₃ / /0.1M LiClO ₄ /	25	-0.14, 0.17 0.51	Pt	19
I ⁻ / I ₂ /	MeCN	Ag/0.1M AgNO ₃ / /0.1M TBABF/	—	-0.20, 0.225 0.68	Pt	a
—	—	Ag/AgCl, LiCl/ /0.1M TBABF/	—	0.30, 0.775 1.18	Pt	a
I ₂ / I ⁻ /	MeCN	Ag/0.1M AgNO ₃ / /0.1M TEAP/	—	0.33, 1.11	PGE	23

a. the present work.

TEAP-Tetraethylammonium perchlorate.

PGE-Pyrolytic graphite Electrode.

TBABF-Tetrabutylammonium Fluoroborate.

3.2.4 Iodide-Iodine Voltammetry in Pyridine

Based on the experimental data in Table 7 and Figure 8, better data are obtained using Ag/0.1M AgNO₃ as a reference electrode than using Ag/AgCl, LiCl. We therefore, selected Ag/0.1M AgNO₃ for all additional experiments. DC and differential pulse polarography cannot be used at high concentrations of electro-active species because currents are too high to measure. It is also observed experimentally that well-defined waves are destroyed by a high pyridine concentration in DC and differential pulse polarography. Cyclic voltammetric measurements were, therefore, employed. A current-voltage plot for 0.00103M N(Bu)₄I at 0 rpm on Pt electrode at a scan rate of 10mv/sec using a 0.1M N(Bu)₄BF₄ supporting electrolyte in pure pyridine show two anodic steps (lower curve, Figure 9). The Polarographic data obtained are given in Table 10. According to the E_{1/2} value shown in Table 10, the first step I₁ is the direct oxidation of iodide to iodine without passing through triiodide ion. This conclusion is in agreement with Iwamoto²⁴. The second step is expected to be in the oxidation of iodine to iodine(I). Interestingly, the absence of Wave II which involves triiodide ion can be explained by the fact that I₃⁻ is not stabilized in the range of 0.001M iodine concentration in pure pyridine. This corresponds to conclusions based on our UV-Vis spectral data which will be discussed later. When the same amount of iodine as iodide

ion is added into the iodide-pyridine solutions, the three anodic steps with $E_{1/2}$ values of about 0.22, 0.54 and 0.95 volt vs SCE occur (upper curve, Figure 9) which is in agreement with Iwamoto²⁴. The $E_{1/2}$ values in Table 10 can be calculated as follow²⁵:

$$E_{1/2} = (E_{p,a} + E_{p,c})/2 \quad (23)$$

Data obtained from measurements using a high concentration of iodine, 0.0802M, in pure pyridine, for fresh and stored solutions, are shown in Figure 10. Two anodic steps and one cathodic step are observed. These steps are similar to those in Figure 8 but not as well defined. The polarographic data are also given in Table 10. The lower curve in Figure 10 for a stored PyI_2 solution, shows that the height of Wave II, which involves the triiodide ion is higher than Wave II in the upper curve for fresh PyI_2 solution. This observation is in agreement with our electrochemical data which show the concentration of triiodide ion increases with time. Also, the presence of Wave I and Wave II in Figure 10, as compared to their absence in Figure 9 indicates triiodide ion is stabilized only in the range of about 0.1M iodine concentration in pure pyridine. This is also in qualitative agreement with our UV-Vis spectral data which we will discuss later. Interestingly, we also find similar results as above for iodine in a mixture of 80% pyridine and 20% n-heptane solutions.

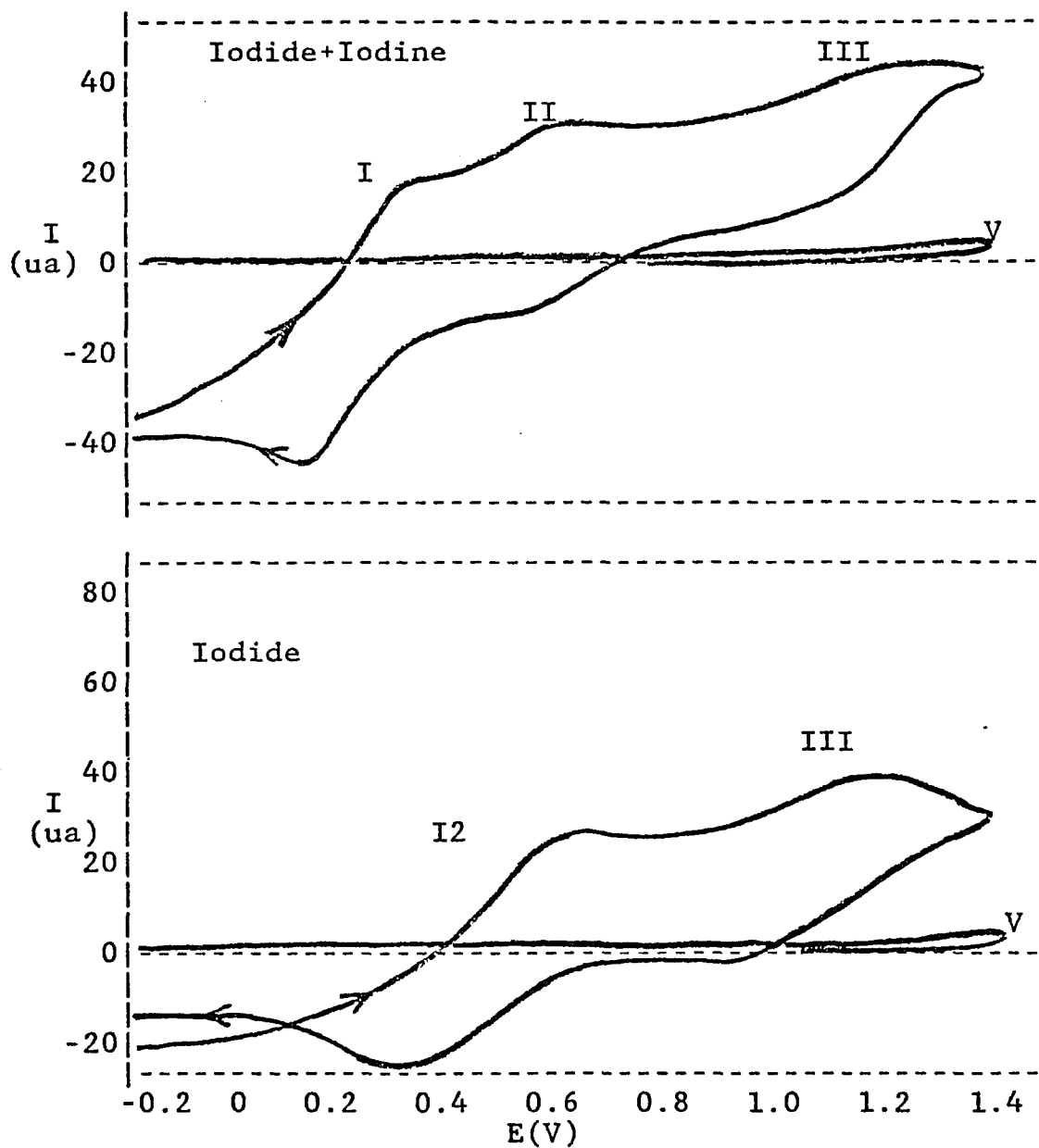


Figure 9: Cyclo-Voltammetry of 0.00103M iodide ion and 0.001M iodine in pyridine for the upper curve. The lower curve: only for 0.00103M iodide ion.
 Wave I for triiodide = iodide.
 Wave II for triiodide = iodine.
 Wave III for iodine = iodine(I).
 Wave I2 for iodide = iodine. V:Residual curve.

TABLE 10
Polarographic Data for Iodide-Iodine

Compound	Solvent	Reference system	Temp. °C	$E_{1/2}$ (V)	Working electrode	Ref.
I^-	Pyridine	Ag/0.1M $AgNO_3$ / /0.1M TBAFB/	25	0.40,0.95	Pt	a
—	—	SCE /0.1M $NaClO_4$ /	—	0.37,0.89	Pt	24
I^- / I_2	Pyridine	Ag/0.1M $AgNO_3$ / /0.1M TBAFB/	25	0.18,0.50 0.91	Pt	a
—	—	SCE /0.1M $NaClO_4$ /	—	0.35,0.50 0.90	Pt	24
I_2	Pyridine	Ag/0.1M $AgNO_3$ / /0.1M TBAFB/	25	-0.01,0.705 1.10 ^b	Pt	a

a.the present work. b.actually is E_p not $E_{1/2}$

TBAFB-Tetrabutylammonium Fluoroborate.

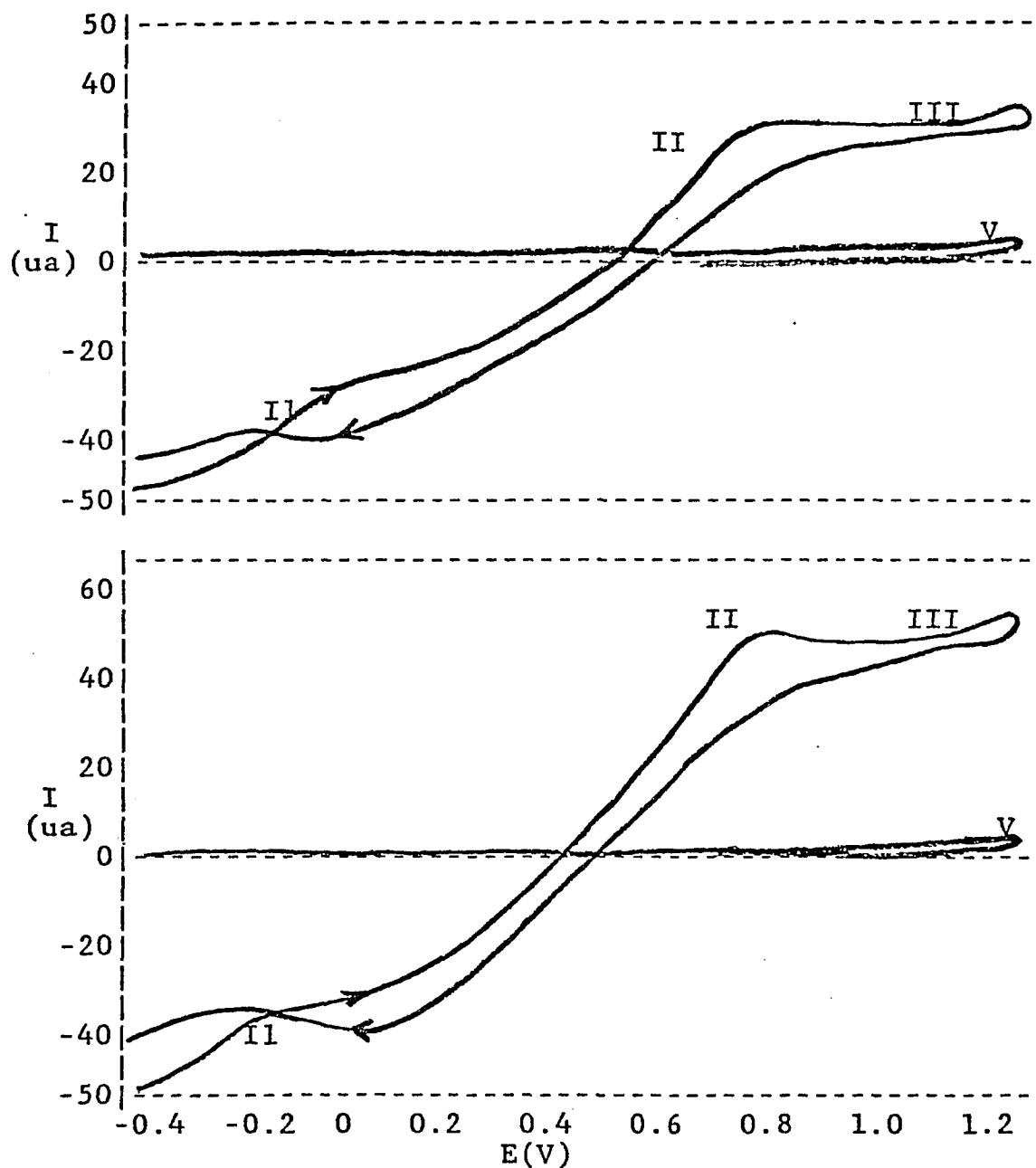


Figure 10: Cyclo-Voltammetry of 0.0802M iodine in pyridine
V-Residual curve. The upper curve for Fresh
solution.

The lower curve for 8 days stored solution.

Wave II for triiodide = iodide.

Wave II for triiodide = iodine.

Wave III for iodine = iodine(I).

3.3 SPECTRAL MEASUREMENTS

A number of spectroscopic studies have been made of charge-transfer complexes with iodine as the acceptor. These studies have been extensively reviewed by Person and Mulliken²⁶ and by Tamres and Yarwood²⁷.

In this section, we present spectral data on pyridine-iodine complexes with the iodine concentration in the range 0.1M to 1.0M which corresponds to the iodine range in the electrochemical measurements. Raman measurements can be made at these high iodine concentration. A 0.01cm cell was used for the UV-Vis measurements.

3.3.1 Raman scattering measurements

Raman spectroscopic measurements on fresh (full line) and 8 days old (broken line) pyridine-iodine solutions with the iodine concentration 0.318M show three major bands (upper curve, Figure 11). The Raman spectrophotometer uses the Ar 488nm line for excitation.

A strong band at 110cm^{-1} and a weak band at 220cm^{-1} are due to symmetric stretching of the triiodide ion and the first overtone, which is in agreement with data on triiodide ion in methanol obtained by Kaya²⁸ and triiodide ion in water obtained by Bernstein²⁹. The other weak band, at 168cm^{-1} , is due to an N-I stretching mode of the pyridine-iodine complex. This is also in agreement with the Raman spectra of iodine charge transfer complexes in solutions obtained by Klaboe³⁰. To establish the origin of these bands, a 0.064M PyI_2 solution in n-heptane and a 0.001M solution of iodine with iodide ion in acetonitrile were examined. The former spectrum shows a single band at 167cm^{-1} , the lower frequency band being absent. The latter spectrum shows two bands, at 112cm^{-1} and 224cm^{-1} . For comparison, pure heptane, pure acetonitrile and iodide ion in acetonitrile have no absorption throughout this range.

When a 0.0159M concentration of iodide ion is added into the solution, the same three bands remain but have different intensities (see Figure 11, lower curve).

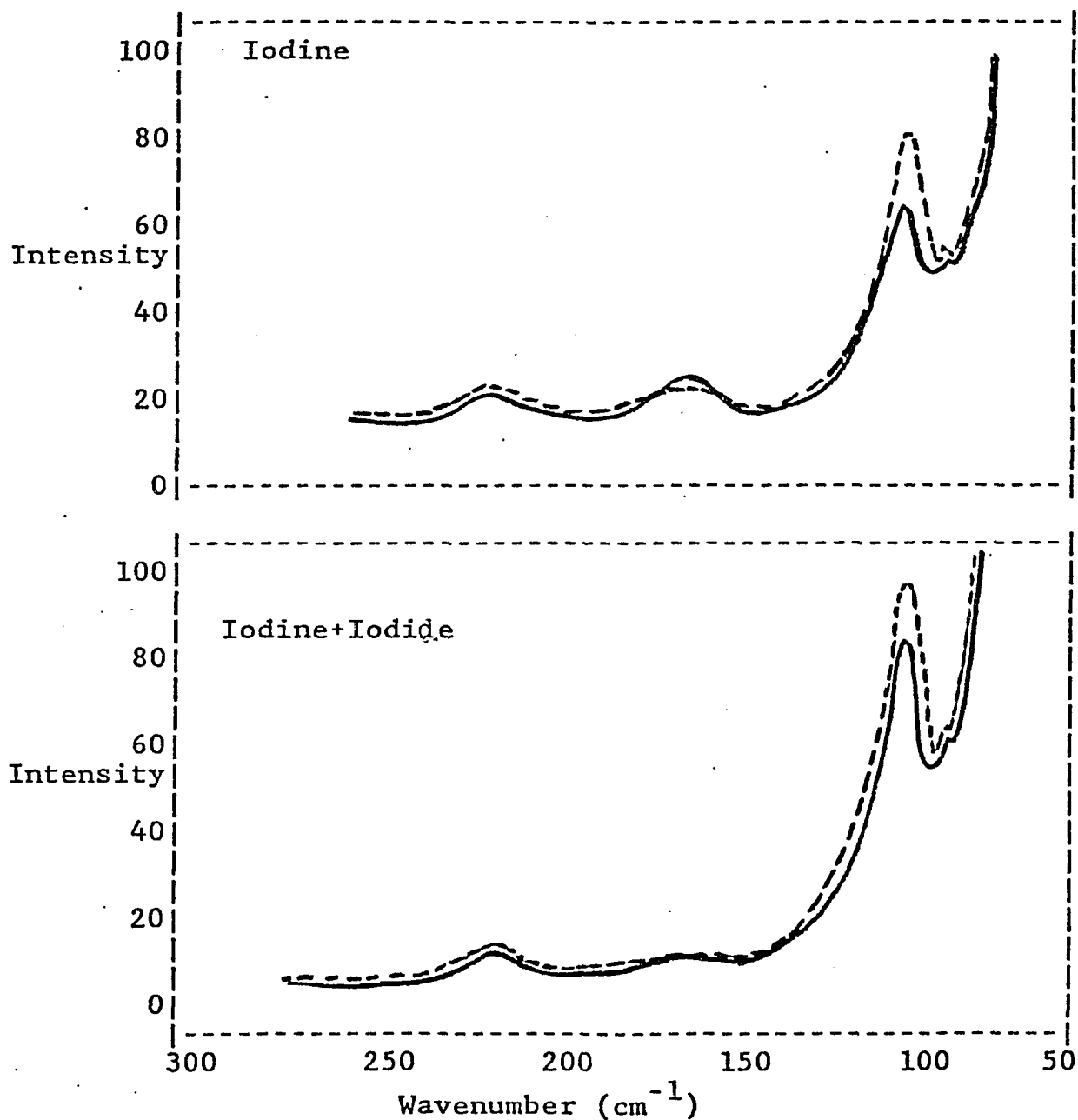
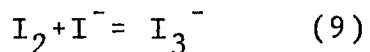


Figure 11: upper curve: Raman spectroscopy of 0.318M iodine, fresh (full line) and stored (broken line) in pure pyridine.
lower curve: 0.159M iodide ion has been added to a fresh solution and measurements made on fresh and stored solutions.

The 110cm^{-1} band increased and the 168cm^{-1} band decreased considerably, indicating a shift of the equilibrium of Reaction 9 to the right.



It is of interest that the 110cm^{-1} band increased in intensity with time (see broken line in Fig. 11), indicating an increasing amount of the I_3^- ions which is in agreement with our previous voltammetry measurements.

3.3.2 UV-Vis absorption measurements

UV-Vis spectrophotometric studies had been made on solutions of iodine in pyridine by Kleinberg^{6,31}. In a continuation of his previous work⁶, the absorption peak in the region of 320nm, reported for pyridine solutions of both iodine and compounds containing the unipositive iodine-pyridine complex, could not be reproduced³¹. Instead, Kleinberg claimed that there occurs in this region a marked increase in absorption, suggesting the existence at a still shorter wavelength of a peak which cannot be located because of the strong absorption of pyridine itself. Our data indicate that this conclusion is only true for low iodine concentration. At high iodine concentration we observed a band at 300nm in the same region as a band is observed for monopyridine iodine(I) chloride and dipyridine iodine(I) nitrate. The reason for the difference between low

and high iodine concentrations may be that the polarization of the complex may vary with iodine concentration, presumably owing to interactions between neighboring $I^+ - I_3^-$ ion-pairs. Interestingly, Toyoda and Person³² found that polarization of the pyridine-iodine complex increased linearly with increasing mole fraction of iodine. Based on the electrostatic model for complex formation, Dewar and Thompson³³ predict an increasing dipole moment with increasing polarizability of the component. This suggests that high iodine concentration will increase the dipole moment of the solution and change pyridine itself to yield an absorption peak in the range below 305nm which will be interfered with another pyridine peak. The dipole moments of pyridine and of PyI_2 in n-heptane are 2.28D and 4.5D as reported by Wantig³⁴ and Carlsohn³⁵.

3.3.2.1 Absorption measurements in pure pyridine

In Figure 12, data are presented on the variation with time of the molar absorptivity of a 0.0785M iodine solution in pyridine. The molar absorptivity for all the data in Figures 12 through 15 is defined as the absorbance per cm per molar concentration of iodine.

The absorption peak of the pyridine iodine complex at 367nm reached a maximum at a peak intensity $e_{\max} = 16,000$ after 6

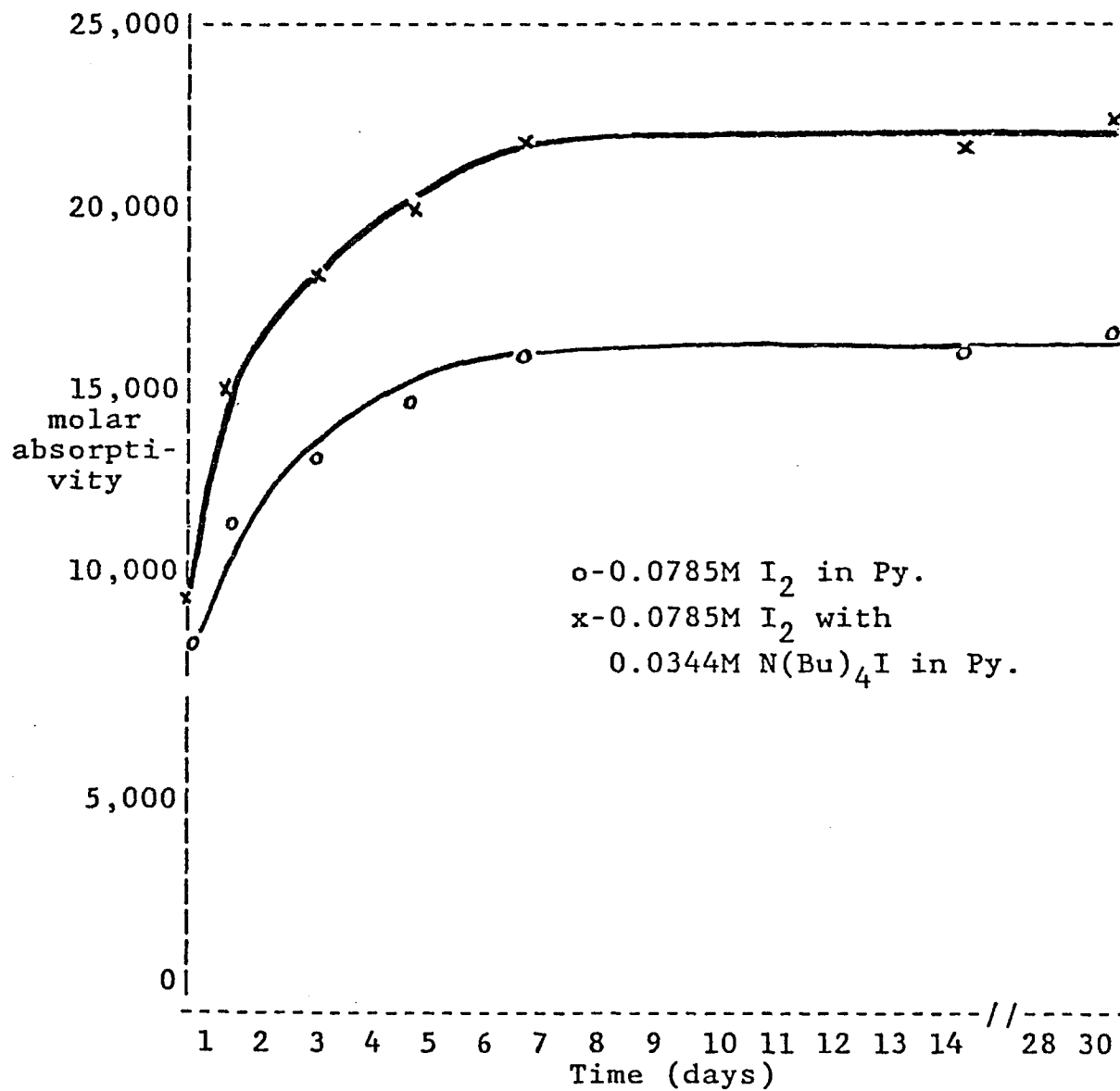


Figure 12: Variation of molar absorptivity of iodine at 367nm with time in pure pyridine.

days, then was constant over a period of 2-4 weeks. This result is in agreement with our ionization data obtained from the electrochemical measurements. The upper curve in Figure 12, for which 0.0344M $N(Bu)_4I$ had been added to the iodine, has a peak intensity $e_{\max} = 22,000$.

UV-Vis spectra were also obtained for iodine concentrations of 0.085M, 0.0085M, 0.00037M and 0.000032M. Significant changes were observed as a function of iodine concentration.

The highest concentration of iodine, 0.085M, and the lowest concentration of iodine, 0.000032M, show different absorption peaks (Figure 13). The lower curve, for the lowest iodine concentration, shows a single band at 422nm which is in agreement with the data on 0.0005M PyI_2 in n-heptane observed by Mulliken³. The 422nm band has been ascribed by Mulliken to the outer-complex of PyI_2 . A gradual rise in molar absorptivity with time is observed (broken line in Figure 13). This change will be discussed in chapter IV. An I_3^- peak is not observed at these low iodine concentration, where I^- , rather than I_3^- , is probably present. The absence of an I_3^- peak is in agreement with our cyclic voltammetric data (page 43).

The upper curve, in Figure 13, for 0.0850M I_2 , shows two bands, at 367nm and 298nm (The usual absorption spectrum of

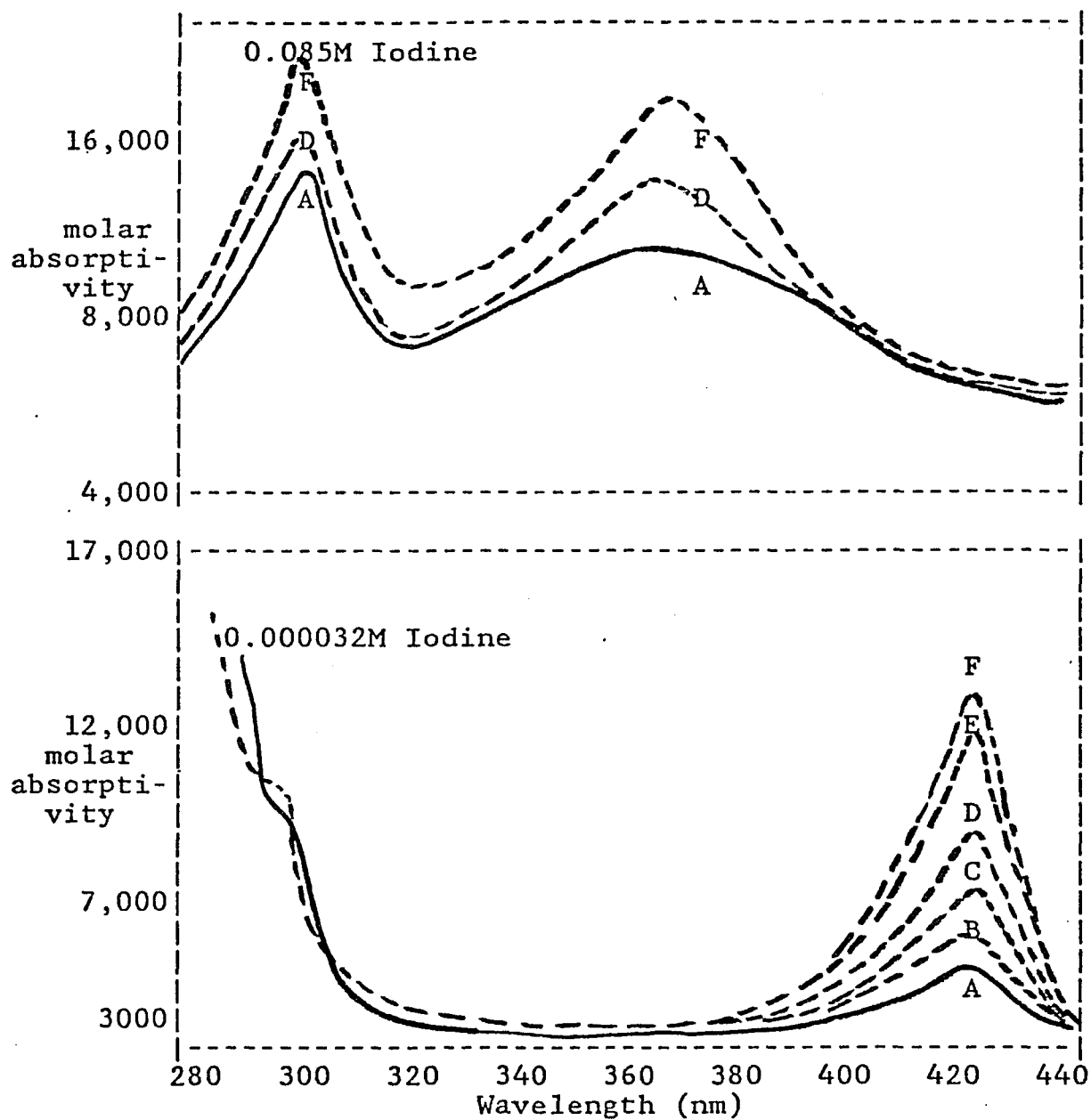


Figure 13: upper curve: UV-Vis spectroscopy of 0.085M iodine, fresh (full line) and stored (broken line) in pure pyridine.
 lower curve: 0.000032M I_2 in pure pyridine.
 A: 0 hr; B: 12 hr; C: 1 day; D: 3 days; E: 5 days; F: 7 days.

I_3^- consists of two bands, one at approximately 365nm and one of nearly double intensity at 295nm³⁶). For a fresh solution of iodine in pyridine, the first band is very broad, has a maximum at 373nm and a peak intensity $e_{\max} = 8000$. This broad band is considerably narrower after one week and the peak maximum has shifted to 367nm. This data will be discussed in a further section. This peak is attributed to the I_3^- ion. This observation is in agreement with our voltammetric polarography (Figure 10) which showed the reduction and oxidation of triiodide ion at 0.0802M I_2 in pyridine. For comparison, we made spectroscopic measurements on 0.0850M monopyridine iodine chloride and dipyridine iodine nitrate in pyridine. These solutions show a single band at 299-302nm and a peak intensity $e_{\max} = 1200$. For these compounds, this band can be attributed either to the undissociated molecules Py_2INO_3 and $PyICl$ or to the dissociated ions PyI^+ or Py_2I^+ . In our case, the band at 300nm may, thus, be attributed to the PyI_2 molecular complex and/or to the ions PyI^+ or Py_2I^+ . A study of 0.003M PyI_2 in acetonitrile shows two bands, at 367nm and 299nm, which are due to I_3^- ion and do not increase in intensity with time.

A 0.0085M concentration of iodine in pyridine, freshly prepared, has an absorption band at at 367nm and 299nm (Full line in Figure 14, top). A 0.00037M concentration of iodine in pyridine has an absorption band at 367nm and a band at about 300nm which is overlapped by a strong band due to

pyridine itself (Full line in Figure 14, bottom). The absorption bands for these two intermediate concentrations shift with time resulting in the presence of a single band at 422nm. The shift occurs much more rapidly in the 0.00037M solution than in the 0.0085M solution. These observations indicate that triiodide ion is not stable in the range of iodine concentrations up to 0.01M. This conclusion is in agreement with our polarographic measurements (the lower curve in Figure 9).

3.3.2.2 Absorption measurements in mixtures of pyridine with n-heptane

Absorption data for iodine in mixtures of pyridine with n-heptane are shown in Figure 15. The absorption band for triiodide ion occurs at the same wavelength as in pure pyridine, 367nm. The e_{\max} value of 12,000, obtained after storing the sample for 6 days, is smaller than in pure pyridine after the same time interval.

The data in Figure 15 show that the absorption for the more concentrated iodine solutions levels off after approximately one week in agreement with the data on pure pyridine. This corresponds to the fact that the percentage ionization of the pyridine-iodine complex remains constant after about a week.

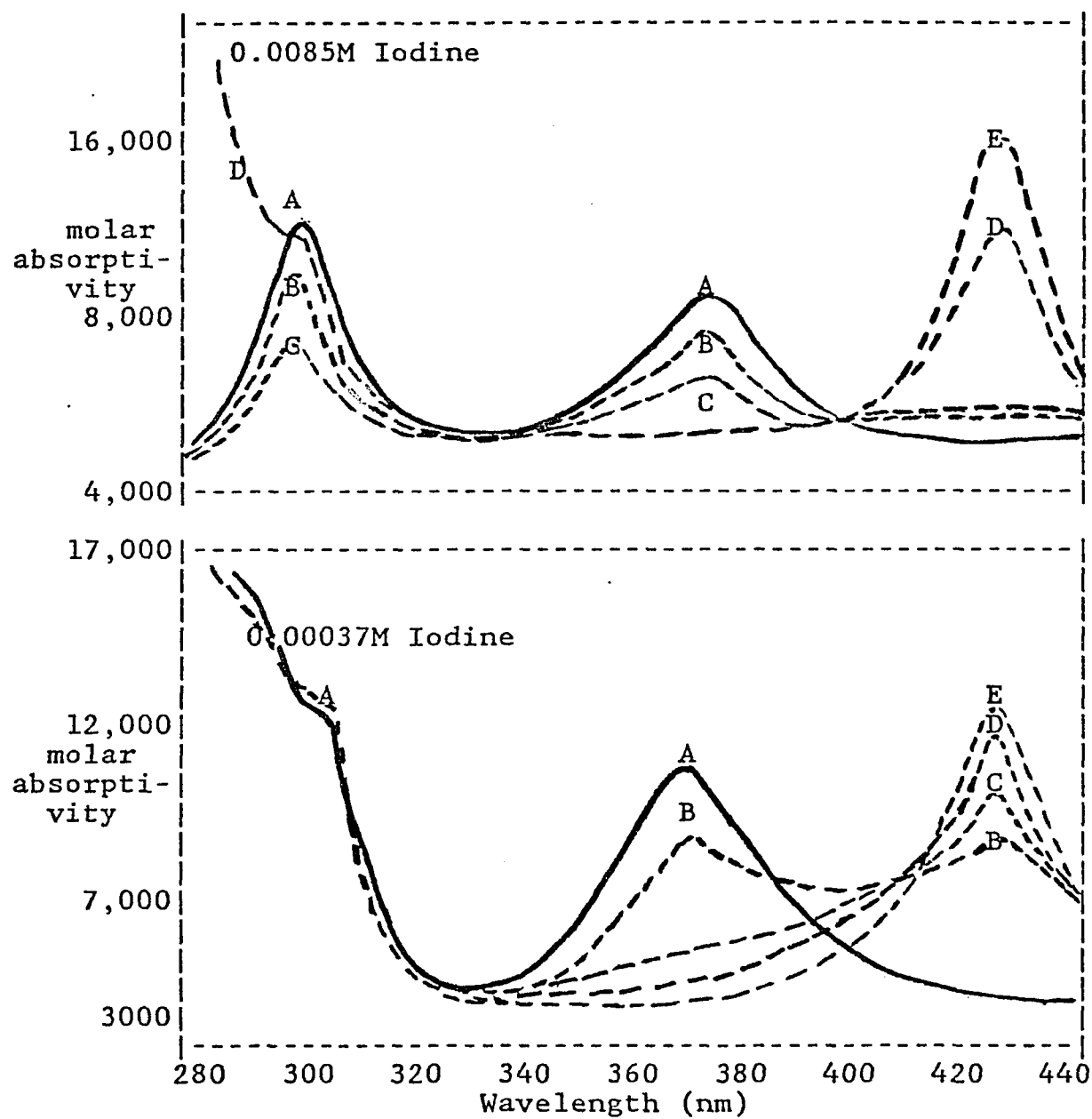


Figure 14: upper curve: UV-Vis spectroscopy of 0.0085M iodine, fresh (full line) and stored (broken line) in pure pyridine.
 lower curve: 0.000037M I_2 in pure pyridine.
 A: 0 hr; B: 2 hr; C: 1 day; D: 5 days; E: 7 days.

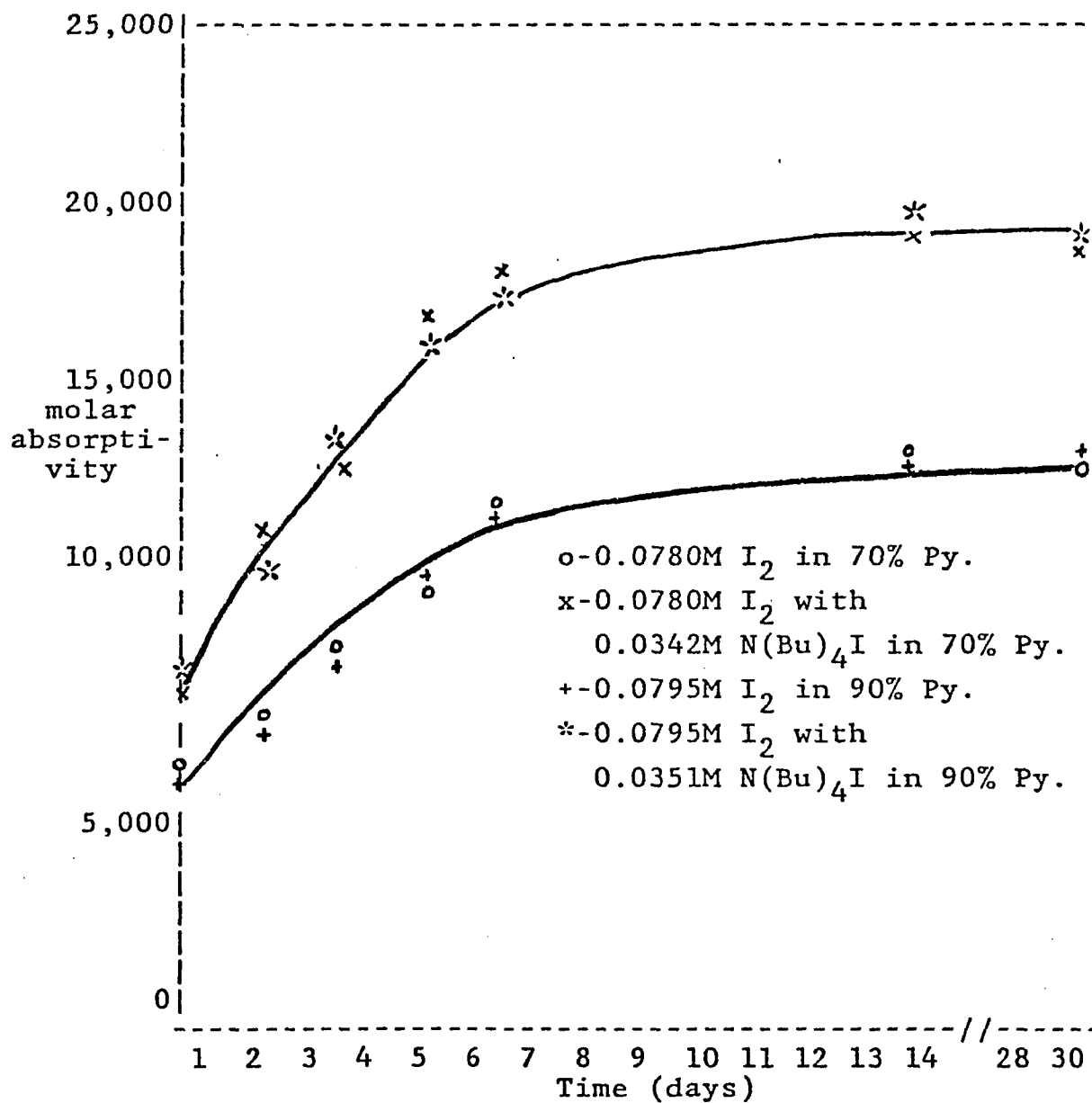


Figure 15: Variation of molar absorptivity of iodine at 367nm with time in mixtures of pyridine and heptane.

In Figure 16, a comparison is made between the UV-Visible spectrum of various pyridine-heptane mixtures for a dilute iodine solution, 0.00045M. In the freshly prepared solutions, there is a gradual shift in the positions of bands with composition. At 1% pyridine, a band appears at 422nm corresponding to the presence of the PyI_2 outer complex, whereas for 100% pyridine having a higher dielectric constant, a band appears at 367nm corresponding to the presence of triiodide ion. After storage for one week, only the band at 422nm is present for all the mixture. This confirms the previously noted lack of stability of triiodide ion at low iodine concentrations.

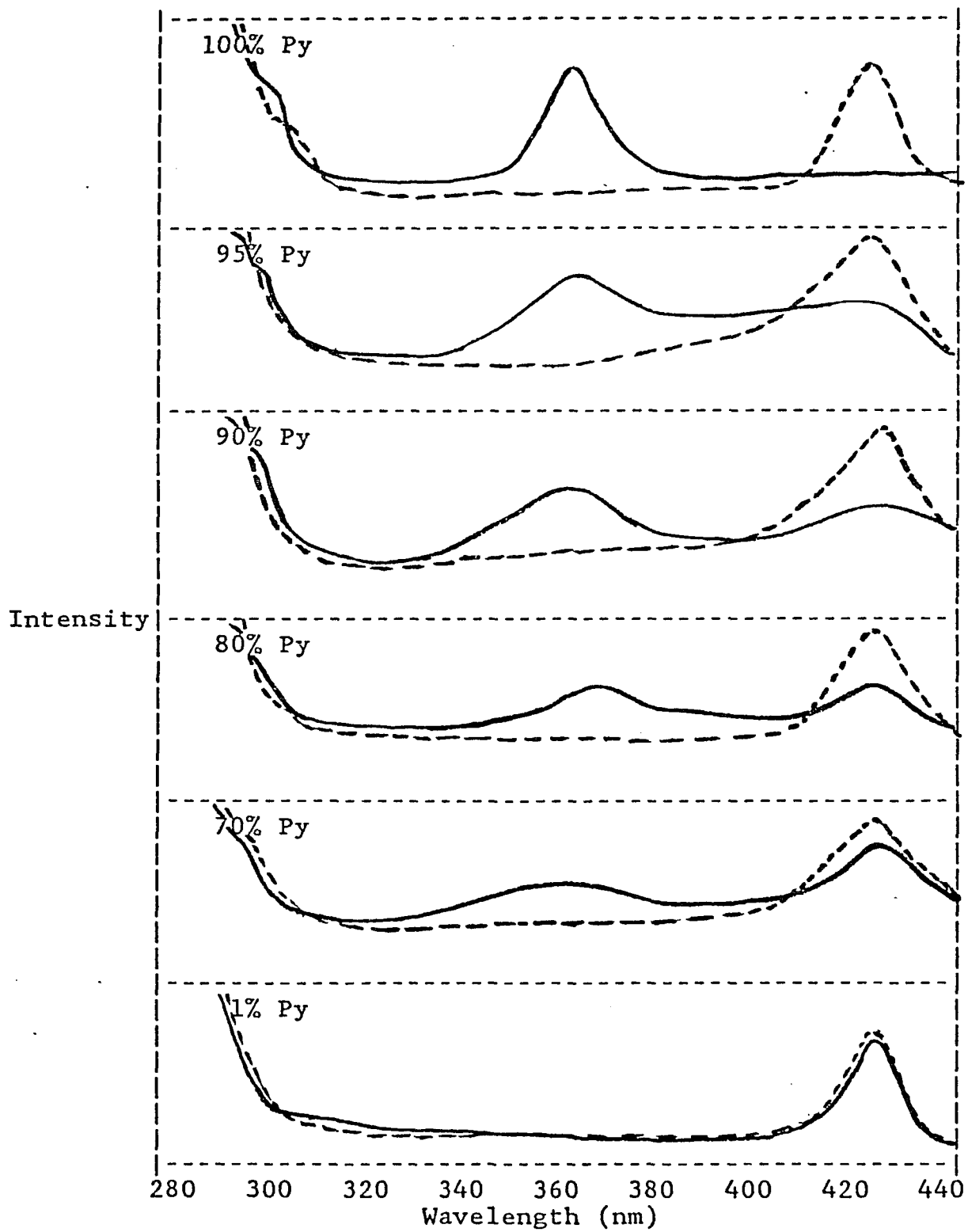


Figure 16: UV-Vis spectroscopy of 0.00045M iodine, fresh (full line) and stored (broken line) in mixtures of Pyridine with heptane.

3.4 CONDUCTIVITY AND I₂ CONCENTRATION CELL MEASUREMENTS

3.4.1 Conductivity measurements

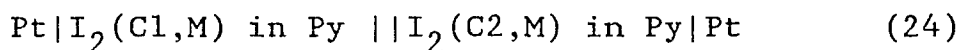
Conductivity data were obtained on the range of iodine concentrations for which electrochemical measurements were made. The data for iodine in pyridine are summarized in Table 11 and Figure 17 for fresh and stored samples. The conductivity is observed to increase with increasing concentration and time as would be expected from the electrochemical data. However, a linear dependence of conductivity on iodine concentration, as would be expected from the electrochemical cell measurements, is not observed. Also, the conductivity of samples stored for more than one week does not level off but continues to increase significantly with time. Audrieth and Birr¹ have also reported that the electric conductivity of iodine in pyridine increases with iodine concentration and with time. It is, therefore, evident that chemical processes are occurring in the pyridine-iodine solutions which are not directly related to the formation and ionization of the pyridine-iodine complex. Audrieth and Birr¹ have suggested the occurrence of irreversible degradation reactions which may produce doubly ionized species such as Py⁺⁺.

The conductivity data for iodine in pyridine-heptane mixtures are summarized in Table 12 and Figure 18. The data for the pyridine-heptane mixtures are consistent with data

in pyridine. The conductivity increases with increasing pyridine content, increasing iodine concentration and time.

3.4.2 I₂ concentration cell measurements

I₂ concentration cell measurements were made at 25°C on electrochemical cells of the type:

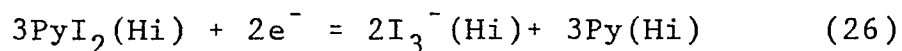
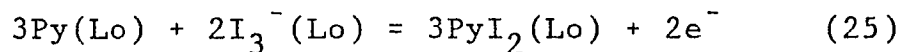


where C1 and C2 are different nominal concentrations of iodine. All the cells used an intermediate compartment containing 0.3M (C₂H₅)₄N⁺Py⁻ in pyridine-iodine solutions. The data obtained are shown in Table 13. Two types of experiment were performed. In the first type of experiment, for which the results are listed in the third column of Table 13, the cell voltage was measured after both iodine solutions had been stored for one week and had been placed in their respective half-cell compartments. In the second type of experiment (column 4 in Table 13), a 1.261M I₂ solution was stored for one week and was diluted to each of the two selected concentrations immediately prior to the EMF measurements.

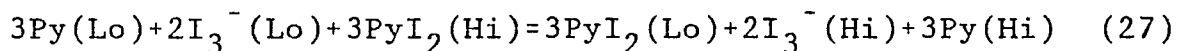
Steady EMF readings were obtained for a period of two and one half hours for all cells. The EMF values were internally consistent. For example, the cell containing I₂ concentrations of 0.0394M and 0.157M gave an EMF value 50.7mv close to the sum of the EMF value for the cell

containing I_2 concentrations of 0.0394M and 0.0788M and the cell containing I_2 concentrations of 0.0788M and 0.157M, 50.1mv.

A theoretical expression for the EMF of the iodine concentration cells can be derived on the assumption that the mechanism expressed in Reactions 12 and 13 are pertinent. For that mechanism, assuming that the pyridine-iodine complex is PyI_2 , we can write



where the oxidation reaction occurs on the side of the cell containing a lower iodine concentration. The overall reaction is



The expression for $EMF_{calc.}$ that is obtained using Reactions 27, 11 and assuming that the ionized pyridine-iodine species is Py_2I^+ is

$$EMF_{calc.} = 0.059/2 \log \frac{PyI_2(Hi)Py^3(Lo)}{PyI_2(Lo)Py^3(Hi)} \quad (28)$$

The EMF values calculated using Equation 28 are shown in the final column in Table 13. The agreement between the experimental and theoretical values is poor except at the highest iodine concentrations. The discrepancies indicate that chemical processes other than those discussed above must also be occurring in the solutions. These results together with the conductivity data indicate the complexity of the pyridine-iodine system.

I_2 concentration cell data obtained in pyridine-heptane mixtures are shown in Table 14. The data are qualitatively similar to those obtained in pure pyridine.

TABLE 11

Summary of data from conductivity cells

I_2 , nominal	$\sigma_0 \times 10^3$	$\sigma_1 \times 10^3$	$\sigma_2 \times 10^3$	$\sigma_3 \times 10^3$
Concn, M	$\text{ohm}^{-1} \text{cm}^{-1}$	$\text{ohm}^{-1} \text{cm}^{-1}$	$\text{ohm}^{-1} \text{cm}^{-1}$	$\text{ohm}^{-1} \text{cm}^{-1}$
0.0197	-----	0.32	0.38	0.45
0.0197	-----	0.31	0.36	0.44
0.0394	-----	0.44	0.53	0.60
0.0411	-----	0.47	0.55	0.61
0.0788	0.18	0.67	0.82	0.91
0.0772	0.15	0.65	0.80	0.92
0.1575	0.38	1.20	1.75	1.93
0.1574	0.39	1.18	1.70	1.90
0.315	0.62	1.77	2.44	3.15
0.310	0.60	1.78	2.50	3.18
0.629	1.43	2.55	4.53	6.03
0.628	1.42	2.65	4.50	6.01
1.257	3.12	4.15	6.15	8.22
1.261	3.14	4.25	6.18	8.23

σ_0 , fresh solution.

σ_1 , stored one week.

σ_2 , stored two weeks.

σ_3 , stored four weeks.

TABLE 12

Summary of conductivity data on iodine dissolved in
pyridine-heptane mixtures

I_2 , nominal Concn, M	$\sigma_1 \times 10^3$ $\text{ohm}^{-1} \text{cm}^{-1}$	$\sigma_2 \times 10^3$ $\text{ohm}^{-1} \text{cm}^{-1}$
0.0397 ^a	0.40	0.44
0.0407 ^b	0.38	0.41
0.0387 ^c	0.30	0.36
0.0378 ^d	0.18	0.29
0.0805 ^a	0.62	0.71
0.0795 ^b	0.54	0.61
0.0787 ^c	0.38	0.55
0.0798 ^d	0.24	0.38
0.152 ^a	0.96	1.02
0.159 ^b	0.84	0.95
0.158 ^c	0.68	0.80
0.159 ^d	0.35	0.52
0.311 ^a	1.58	1.85
0.314 ^b	1.31	1.50
0.315 ^c	1.10	1.22
0.311 ^d	0.71	0.91
0.633 ^a	2.30	3.32
0.631 ^b	2.02	2.78
0.630 ^c	1.65	2.12
0.633 ^d	1.25	1.58
1.257 ^a	4.05	5.25
1.259 ^b	3.90	4.95
1.261 ^c	3.30	4.65
1.261 ^d	2.26	2.85

a. In 95% Py. and 5% Hep. system. Dielectric constant=11.83.

b. In 90% Py. and 10% Hep. system. Dielectric constant=11.31.

c. In 80% Py. and 20% Hep. system. Dielectric constant=10.26.

d. In 70% Py. and 30% Hep. system. Dielectric constant=9.22.

σ_1 , stored one week.

σ_2 , stored two weeks.

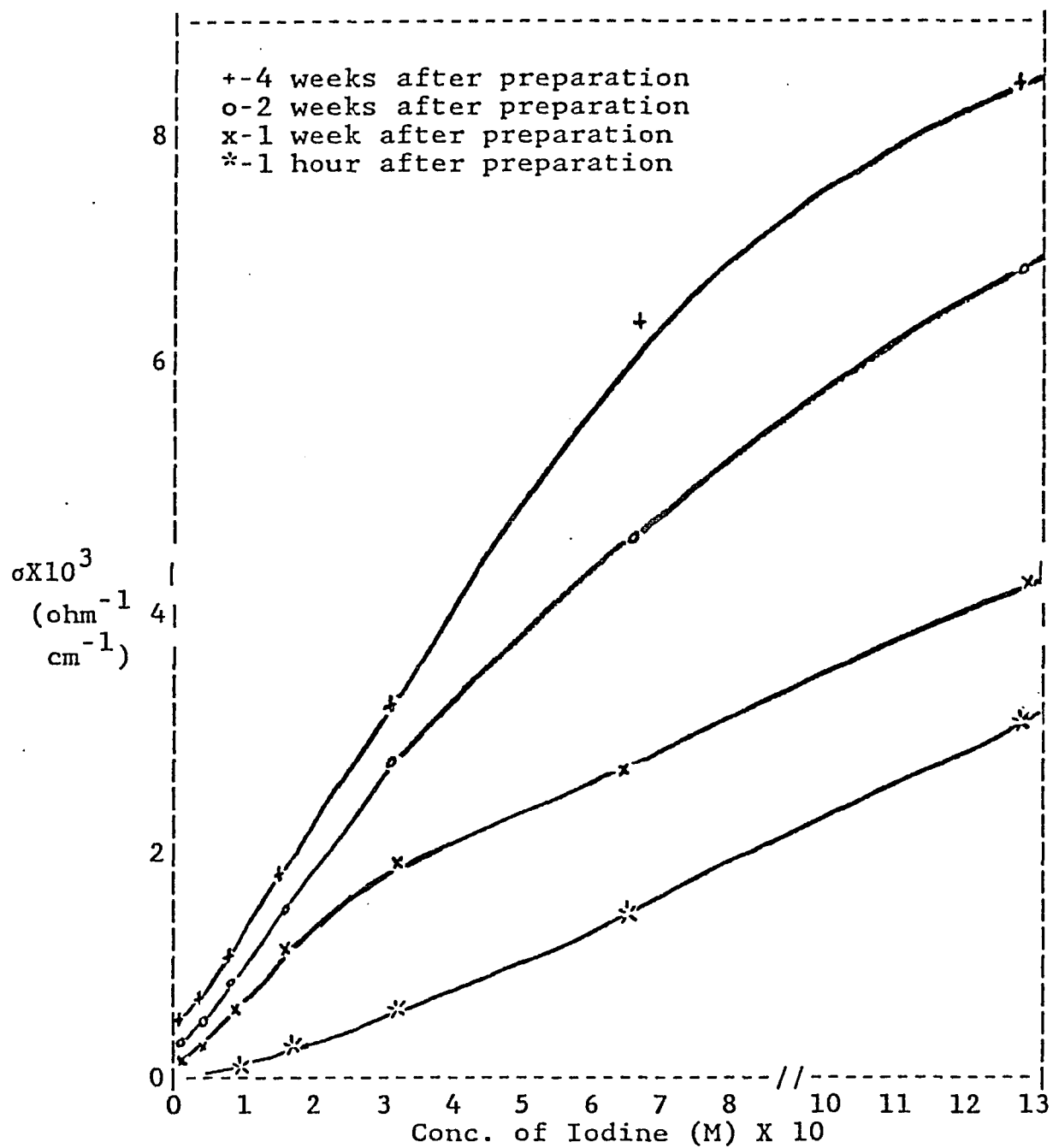


Figure 17: Variation of specific conductivity with iodine concentration and storage time for pure pyridine solutions.

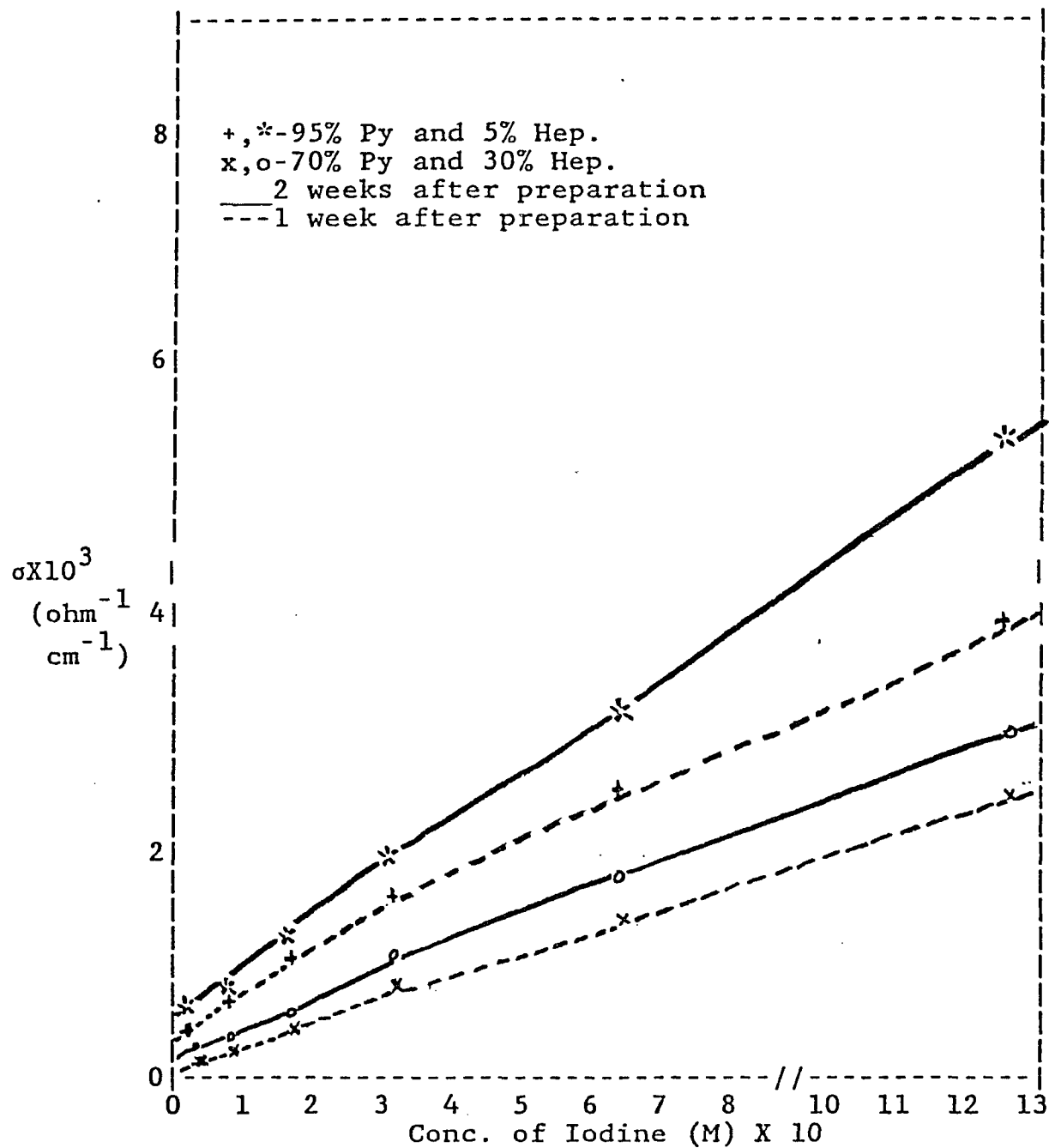


Figure 18: Variation of specific conductivity with iodine concentration and storage time for pyridine-heptane mixtures.

TABLE 13

EMF data on the cell $\text{Pt}|\text{I}_2(\text{C1},\text{M})$ in $\text{Py}||\text{I}_2(\text{C2},\text{M})$ in $\text{Py}|\text{Pt}^{\text{a}}$

C1,M	C2,M	EMF _{exp.1} ,mv	EMF _{exp.2} ,mv	EMF _{calc.} ,mv
0.628	1.261	14.5	12.3	12.4
0.317	0.628	16.7	12.8	10.35
0.157	0.317	18.2	15.3	9.47
0.0788	0.157	24.1	14.5	9.44
0.0394	0.0788	26.0	16.6	9.00
0.0394	0.157	50.7	30.7	18.44
0.0394	0.317	68.5	45.5	27.91

a. Oxidation occurs on the side of cell containing a lower iodine concentration.

Exp.1 obtained after one week storage of both components.

Exp.2 obtained after one week storage of the 1.261M stock solution and dilution to the appropriate concentrations.

TABLE 14

EMF data on the cell $\text{Pt}|\text{I}_2(\text{C1},\text{M})$ in Py-Hep|| $\text{I}_2(\text{C2},\text{M})$ in Py-Hep|Pt^e

C1,M	C2,M	EMF _{exp.1} ,mv	EMF _{exp.2} ,mv
0.633 ^a	1.257 ^a	11.2	12.1
0.631 ^b	1.259 ^b	12.5	12.7
0.630 ^c	1.261 ^c	15.4	13.6
0.633 ^d	1.261 ^d	16.2	15.1
0.311 ^a	0.633 ^a	17.8	13.1
0.314 ^b	0.631 ^b	19.0	15.2
0.315 ^c	0.630 ^c	19.2	16.1
0.311 ^d	0.633 ^d	20.2	18.3
0.152 ^a	0.311 ^a	22.4	18.7
0.159 ^b	0.314 ^b	23.2	19.4
0.158 ^c	0.315 ^c	23.0	20.1
0.159 ^d	0.311 ^d	24.5	19.8
0.0805 ^a	0.152 ^a	25.3	19.5
0.0795 ^b	0.159 ^b	23.1	20.7
0.0787 ^c	0.158 ^c	26.9	21.2
0.0798 ^d	0.159 ^d	25.8	22.3
0.0397 ^a	0.0805 ^a	25.9	21.7
0.0407 ^b	0.0795 ^b	26.5	23.8
0.0387 ^c	0.0787 ^c	27.0	22.5
0.0378 ^d	0.0798 ^d	27.1	23.1

a. In 95% pyridine and 5% n-heptane system.

b. In 90% pyridine and 10% n-heptane system.

c. In 80% pyridine and 20% n-heptane system.

d. In 70% pyridine and 30% n-heptane system.

e. Oxidation occurs on the side of cell containing a lower iodine concentration.

Exp.1 obtained after one week storage of both components.

Exp.2 obtained after one week storage of the 1.261M stock solution and dilution to the appropriate concentrations.

Chapter IV

OVERVIEW OF THE PYRIDINE-IODINE COMPLEXATION AND DISSOCIATION REACTIONS

The electrochemical data in section 3.1 together with the spectroscopic data provide us with sufficient information to develop a qualitative picture of the complexation and ionic dissociation reactions in pure pyridine over a wide range of iodine concentrations, 10^{-6} M to 1M, and for a wide range of pyridine-heptane mixtures. Table 15 and 16 summarize the various complexation and ionic dissociation reactions which the data lead us to propose.

For high iodine, the various steps shown in Reaction 29 must occur. The reversible nature of the electrochemical cell indicates that the dissociated ions, Py_2I^+ and I_3^- , are always in dynamic equilibrium with the complex shown as PyI_2^{**} . This complex may correspond to the 'inner complex' PyI^+I^- proposed by Mulliken^{3,10}. The first step in Reaction 29 must be rapid because free I_2 disappears immediately as is evidenced by the absence of an I_2 band, which occurs at about 480-540nm³⁸ in organic solvents. The complex in brackets, PyI_2^* , is never observed but must be present to account for the increase with time of the I_3^- ionic dissociation product. We attribute to the disappearance of

the PyI_2^* the fact that the observed percent dissociation of PyI_2^{**} becomes constant after about one week. The formulas PyI_2^{**} and Py_2I^+ may actually be $\text{Py}_2\text{I}_2^{**}$ and PyI^+ . Our data cannot distinguish between these possibilities.

The spectroscopic data in Figure 14 indicate that at intermediate iodine concentrations, 10^{-4}M to 10^{-2}M , the steps in Reaction 30 are dominant. Both the PyI_2^* and the PyI_2^{**} complexes are slowly converted into PyI_2^{***} which has an absorption band at 422nm. The PyI_2^{***} complex may correspond to the 'outer complex' proposed by Mulliken.

At low I_2 concentrations, there is no spectroscopic evidence for the presence of I_3^- . The PyI_2^{***} absorption band increases significantly with time (Figure 13). The dominance of Reaction 31 is indicated in which the PyI_2^* complex is slowly converted to PyI_2^{***} without going through the PyI_2^{**} stage.

In the case of pyridine-heptane mixtures, the reactions occurring at high iodine concentrations are the same as those occurring in pure pyridine. The electrochemical cell data are very similar to those in pure pyridine. The reaction steps are shown in Reaction 32.

At an iodine concentration of about 10^{-4}M , the spectroscopic evidence (Figure 16) indicates different behavior at high pyridine concentrations (Reaction 33), at

intermediate pyridine concentrations (Reaction 34) and at low pyridine concentrations (Reaction 35). At high pyridine concentrations, PyI_2^{**} is slowly converted to PyI_2^{***} in correspondence with the data in pure pyridine (Reaction 30). At intermediate concentration of pyridine, PyI_2^{***} , as well as PyI_2^{**} , is formed immediately. The concentration of PyI_2^{***} then continues to increase with time. The immediate appearance of PyI_2^{***} indicates that the complex forms directly by the interaction of pyridine and iodine. At low iodine concentrations, all the PyI_2^{***} is formed directly from pyridine and iodine as is evidenced by the fact that the PyI_2^{***} band at 422nm does not increase significantly with time (Figure 16, bottom). In fact, several investigators^{3,5,7,8} have measured the equilibrium constant for the direct reaction between pyridine and iodine to form PyI_2^{***} at low pyridine and low iodine concentrations.

The reasons that the concentration of iodine affects the reactions in the way described above are not clear. The molecular polarization of the various PyI_2 complexes and the I_3^- and PyI^+ complexes may play a role³². The dielectric constant of the solvent system is also an important factor in these reactions³³.

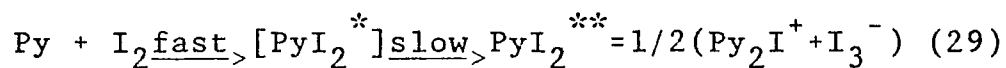
There is, thus, much additional work to be done to further elucidate the nature of the interaction of iodine with pyridine. It should be mentioned once again that the above

mechanisms do not fully account for the I_2 concentration cell data or the conductivity data. This reenforces our conclusion that the pyridine-iodine system is complex.

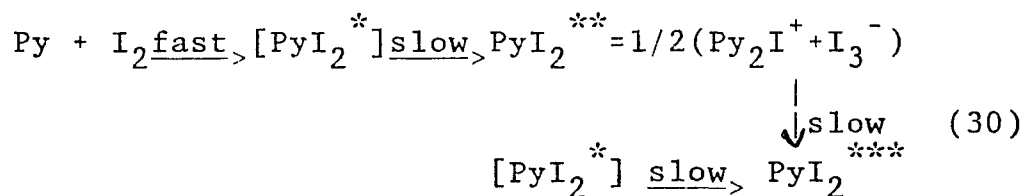
TABLE 15

Pyridine-iodine complexation reactions in pure pyridine

High concentration of iodine ($>10^{-2}\text{M}$)



Intermediate concentration of iodine ($10^{-2}\text{M} - 10^{-4}\text{M}$)



Low concentration of iodine ($<10^{-4}\text{M}$)

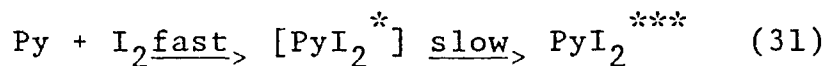
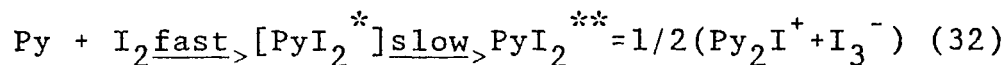


TABLE 16

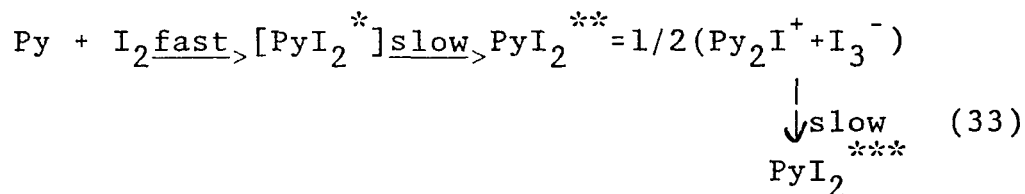
Pyridine-iodine complexation reactions in Pyridine-Heptane
mixtures

High concentration of iodine ($>10^{-2}M$)

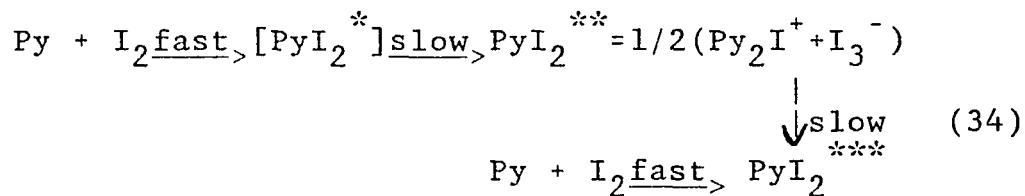


Low concentration of iodine (about $10^{-4}M$)

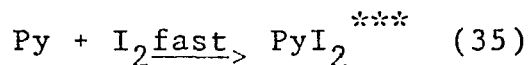
a. high conc. pyridine



b. Intermediate conc. pyridine



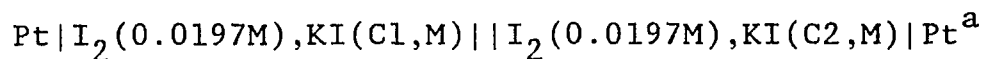
c. low conc. pyridine



Appendix A
EMF data in pure pyridine solutions

TABLE 17

EMF data on the cell



C1,M	C2,M	E,mv	Y1,M	Y2,M	K1,M ²	X,M
0.000825	0.00043	2.90	0.00135	0.00151	0.00000294	0.00171
0.00119	0.00041	5.50	0.00127	0.00158	0.00000313	0.00177
0.00152	0.00038	8.02	0.00115	0.00157	0.00000307	0.00175
0.00182	0.00036	10.08	0.00107	0.00159	0.00000311	0.00176
0.00211	0.00034	12.41	0.00095	0.00155	0.00000292	0.00171

						0.0017 _± 0.0006

0.000778	0.000389	2.67	0.00149	0.00166	0.00000340	0.00184
0.00112	0.000373	5.16	0.00134	0.00164	0.00000329	0.00181
0.00144	0.000359	7.53	0.00120	0.00161	0.00000316	0.00178
0.00173	0.000346	9.75	0.00107	0.00107	0.00000301	0.00173
0.00200	0.000333	11.86	0.00096	0.00153	0.00000286	0.00169

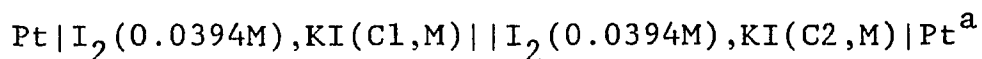
						0.0018 ^b _± 0.0009

a. In pure pyridine.

b. In this cell, the concentration of I₂ was 0.0197M
and NaI, rather than KI, was present in both half-cells.

TABLE 18

EMF data on the cell



C1,M	C2,M	E,mv	Y1,M	Y2,M	K1,M ²	X,M
0.00128	0.000669	1.66	0.00409	0.00437	0.0000220	0.00469
0.00185	0.000641	3.38	0.00370	0.00423	0.0000206	0.00454
0.00237	0.000616	4.70	0.00368	0.00442	0.0000222	0.00471
0.00285	0.000592	5.90	0.00360	0.00453	0.0000232	0.00482
0.00330	0.000570	7.25	0.00334	0.00443	0.0000222	0.00471

						0.0047±0.0001

0.00210	0.00105	2.55	0.00427	0.00472	0.0000272	0.00521
0.00303	0.00101	4.72	0.00408	0.00490	0.0000289	0.00538
0.00388	0.000970	6.73	0.00379	0.00493	0.0000290	0.00539
0.00467	0.000934	8.65	0.00348	0.00488	0.0000284	0.00533
0.00540	0.000901	10.49	0.00319	0.00480	0.0000274	0.00523

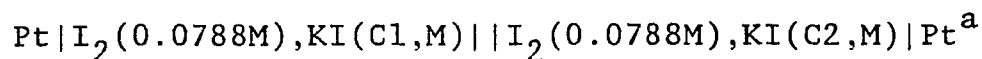
						0.0052 ^b ±0.0001

a. In pure pyridine.

b. In this cell, the concentration of I₂ was 0.0411M
and NaI, rather than KI, was present in both half-cells.

TABLE 19

EMF data on the cell



C1,M	C2,M	E,mv	Y1,M	Y2,M	K1,M ²	X,M
0.00256	0.00133	1.75	0.00776	0.00831	0.0000801	0.00895
0.00368	0.00128	3.20	0.00786	0.00890	0.0000906	0.00952
0.00472	0.00123	4.53	0.00767	0.00915	0.0000949	0.00974
0.00569	0.00118	5.70	0.00752	0.00940	0.0000994	0.00997
0.00658	0.00114	6.87	0.00717	0.00938	0.0000986	0.00993

						0.0096 _± 0.0008

0.00280	0.00140	1.85	0.00834	0.00896	0.0000928	0.00963
0.00403	0.00134	3.50	0.00794	0.00910	0.0000950	0.00975
0.00517	0.00129	4.99	0.00756	0.00919	0.0000963	0.00981
0.00622	0.00124	6.45	0.00707	0.00909	0.0000939	0.00969
0.00720	0.00120	7.71	0.00676	0.00913	0.0000943	0.00971

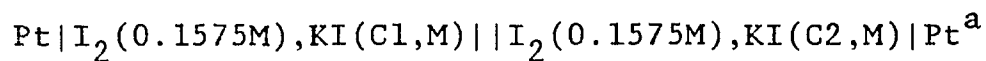
						0.0097 ^b _± 0.0002

a. In pure pyridine.

b. In this cell, the concentration of I_2 was 0.0772M
and NaI, rather than KI, was present in both half-cells.

TABLE 20

EMF data on the cell



C1,M	C2,M	E,mv	Y1,M	Y2,M	K1,M ²	X,M
0.00506	0.00263	1.65	0.0164	0.0175	0.000352	0.0188
0.00730	0.00253	3.24	0.0154	0.0175	0.000349	0.0187
0.00937	0.00243	4.84	0.0140	0.0169	0.000328	0.0181
0.0113	0.00234	6.10	0.0137	0.0173	0.000341	0.0185
0.0131	0.00226	7.15	0.0135	0.0179	0.000360	0.0190

						0.0186 _± 0.0003

0.00547	0.00269	1.99	0.0153	0.0165	0.000316	0.0178
0.00787	0.00258	3.70	0.0146	0.0168	0.000328	0.0181
0.0101	0.00248	5.33	0.0136	0.0168	0.000325	0.0180
0.0121	0.00239	6.80	0.0128	0.0167	0.000320	0.0179
0.0141	0.00231	8.17	0.0122	0.0168	0.000322	0.0180

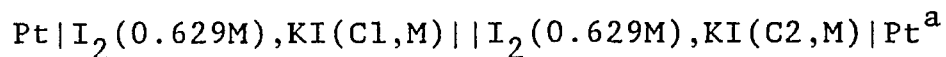
						0.0179 ^b _± 0.0001

a. In pure pyridine.

b. In this cell, the concentration of I₂ was 0.1574M
and NaI, rather than KI, was present in both half-cells.

TABLE 21

EMF data on the cell



C1,M	C2,M	E,mv	Y1,M	Y2,M	K1,M ²	X,M
0.0202	0.0105	1.70	0.0633	0.0676	0.00528	0.0727
0.0291	0.0101	3.16	0.0632	0.0715	0.00583	0.0763
0.0372	0.00968	4.64	0.0586	0.0703	0.00562	0.0750
0.0448	0.00931	5.72	0.0589	0.0737	0.00611	0.0782
0.0519	0.00896	6.82	0.0572	0.0746	0.00624	0.0790

						0.0762 _± 0.0026

0.0229	0.0115	1.95	0.0638	0.0688	0.00553	0.0744
0.0330	0.0110	3.72	0.0602	0.0696	0.00561	0.0749
0.0423	0.0106	5.38	0.0560	0.0691	0.00551	0.0742
0.0510	0.0102	6.82	0.0536	0.0670	0.00561	0.0749
0.0590	0.00983	8.23	0.0504	0.0695	0.00552	0.0743

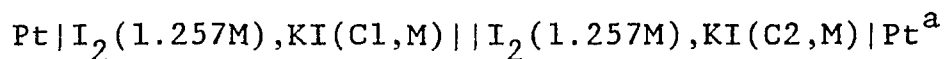
						0.0745 ^b _± 0.0004

a. In pure pyridine.

b. In this cell, the concentration of I₂ was 0.628M
and NaI, rather than KI, was present in both half-cells.

TABLE 22

EMF data on the cell



C1,M	C2,M	E,mv	Y1,M	Y2,M	K1,M ²	X,M
0.0404	0.0211	1.63	0.132	0.141	0.0228	0.151
0.0582	0.0202	3.15	0.127	0.143	0.0235	0.153
0.0746	0.0194	4.55	0.121	0.144	0.0235	0.153
0.0898	0.0186	5.77	0.117	0.146	0.0242	0.155
0.104	0.0180	6.95	0.111	0.146	0.0241	0.155
						0.154 ₊ 0.001
0.0447	0.0224	1.96	0.124	0.134	0.0209	0.145
0.0644	0.0215	3.73	0.117	0.135	0.0212	0.146
0.0826	0.0206	5.04	0.119	0.145	0.0241	0.155
0.0994	0.0199	6.37	0.115	0.147	0.0245	0.157
0.115	0.0192	7.59	0.110	0.148	0.0248	0.158
						0.152 ^b ₊ 0.006

a. In pure pyridine.

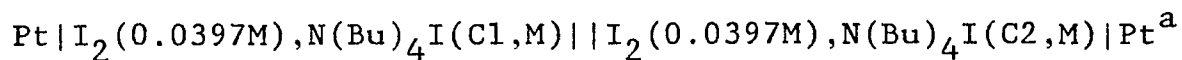
b. In this cell, the concentration of I₂ was 1.261M and NaI, rather than KI, was present in both half-cells.

Appendix B

EMF data in pyridine-heptane solutions

TABLE 23

EMF data on the cell



C1,M	C2,M	E,mv	Y1,M	Y2,M	K1,M ²	X,M
0.00132	0.000658	1.68	0.00441	0.00471	0.0000252	0.00502
0.00189	0.000632	3.23	0.00409	0.00464	0.0000247	0.00495
0.00243	0.000608	4.66	0.00388	0.00465	0.0000245	0.00494
0.00292	0.000585	6.07	0.00359	0.00456	0.0000234	0.00484
0.00339	0.000564	7.34	0.00341	0.00454	0.0000232	0.00482

						0.0049 <u>+</u> 0.0002

0.00139	0.000695	1.72	0.00450	0.00481	0.0000265	0.00515
0.00200	0.000667	3.27	0.00427	0.00485	0.0000268	0.00517
0.00256	0.000642	4.79	0.00394	0.00475	0.0000256	0.00506
0.00309	0.000618	6.12	0.00376	0.00478	0.0000258	0.00508
0.00357	0.000596	7.37	0.00357	0.00476	0.0000255	0.00505

						0.0051 ^b <u>+</u> 0.0002

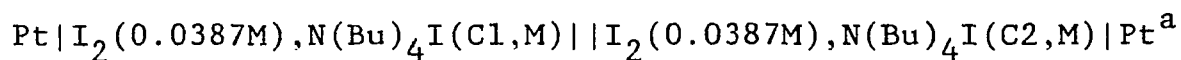
a. In 95% pyridine and 5% n-heptane.

b. In this cell, the concentration of I₂ was 0.0407M

and 90% Py, rather than 95% Py, was present in both half-cells.

TABLE 24

EMF data on the cell



C1,M	C2,M	E,mv	Y1,M	Y2,M	K1,M ²	X,M
0.00137	0.000687	1.76	0.00431	0.00461	0.0000244	0.00494
0.00198	0.000660	3.39	0.00405	0.00462	0.0000244	0.00494
0.00254	0.000634	5.01	0.00369	0.00449	0.0000230	0.00480
0.00305	0.000611	6.41	0.00349	0.00448	0.0000228	0.00477
0.00353	0.000589	7.59	0.00339	0.00455	0.0000234	0.00484

						0.0048 <u>+</u> 0.0002

0.00136	0.000683	1.79	0.00418	0.00449	0.0000232	0.00482
0.00197	0.000656	3.41	0.00400	0.00457	0.0000239	0.00489
0.00252	0.000631	5.12	0.00356	0.00435	0.0000216	0.00465
0.00303	0.000607	6.51	0.00339	0.00437	0.0000218	0.00467
0.00351	0.000586	7.67	0.00332	0.00447	0.0000226	0.00476

						0.0047 ^b <u>+</u> 0.0002

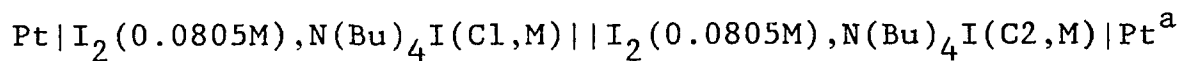
a. In 80% pyridine and 20% n-heptane.

b. In this cell, the concentration of I₂ was 0.0378M

and 70% Py, rather than 80% Py, was present in both half-cells.

TABLE 25

EMF data on the cell



C1,M	C2,M	E,mv	Y1,M	Y2,M	K1,M ²	X,M
0.00294	0.00147	1.73	0.00946	0.0101	0.0001172	0.0108
0.00423	0.00141	3.30	0.00894	0.0102	0.0001177	0.0108
0.00543	0.00136	4.74	0.00847	0.0102	0.0001178	0.0108
0.00653	0.00131	6.20	0.00781	0.00995	0.0001119	0.0106
0.00756	0.00126	7.55	0.00731	0.00981	0.0001087	0.0104

						0.0107 <u>±</u> 0.0002

0.00285	0.00143	1.79	0.00878	0.00941	0.0001021	0.0101
0.00411	0.00137	3.37	0.00847	0.00965	0.0001065	0.0103
0.00527	0.00132	4.86	0.00796	0.00963	0.0001054	0.0103
0.00634	0.00127	6.19	0.00760	0.00968	0.0001060	0.0103
0.00734	0.00122	7.44	0.00725	0.00969	0.0001060	0.0103

						0.0102 ^b <u>±</u> 0.0001

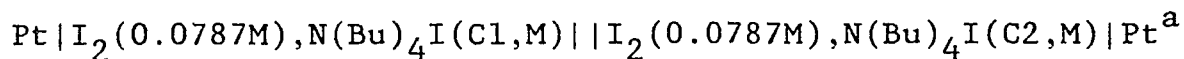
a. In 95% pyridine and 5% n-heptane.

b. In this cell, the concentration of I₂ was 0.0795M

and 90% Py, rather than 95% Py, was present in both half-cells.

TABLE 26

EMF data on the cell



C1,M	C2,M	E,mv	Y1,M	Y2,M	K1,M ²	X,M
0.00278	0.00139	1.70	0.00912	0.00975	0.000109	0.0104
0.00401	0.00133	3.38	0.00826	0.00942	0.000101	0.0101
0.00514	0.00129	4.65	0.00821	0.00985	0.000109	0.0105
0.00618	0.00124	6.02	0.00769	0.00972	0.000107	0.0103
0.00715	0.00119	7.20	0.00739	0.00979	0.000107	0.0104

						0.0104 _± 0.0002

0.00296	0.00148	1.83	0.00892	0.00959	0.000106	0.0103
0.00426	0.00142	3.64	0.00798	0.00920	0.0000977	0.0099
0.00547	0.00137	5.17	0.00763	0.00934	0.000100	0.0100
0.00658	0.00132	6.48	0.00741	0.00955	0.000104	0.0102
0.00761	0.00127	7.73	0.00711	0.00962	0.000105	0.0102

						0.0100 ^b _± 0.0002

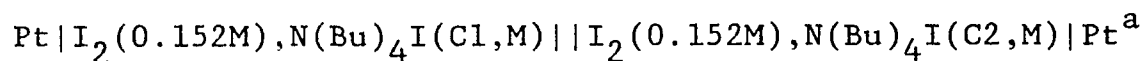
a. In 80% pyridine and 20% n-heptane.

b. In this cell, the concentration of I₂ was 0.0798M

and 70% Py, rather than 80% Py, was present in both half-cells.

TABLE 27

EMF data on the cell



C1,M	C2,M	E,mv	Y1,M	Y2,M	K1,M ²	X,M
0.00535	0.00267	1.84	0.0161	0.0173	0.000344	0.0185
0.00770	0.00257	3.58	0.0147	0.0169	0.000330	0.0182
0.00988	0.00247	5.05	0.0142	0.0173	0.000343	0.0185
0.0119	0.00238	6.50	0.0134	0.0172	0.000338	0.0184
0.0137	0.00229	7.80	0.0126	0.0171	0.000333	0.0182

						0.0183 _± 0.0001

0.00574	0.00287	1.97	0.0159	0.0172	0.000343	0.0185
0.00827	0.00276	3.71	0.0151	0.0175	0.000354	0.0188
0.0106	0.00265	5.35	0.0142	0.0174	0.000350	0.0187
0.0127	0.00255	6.82	0.0133	0.0174	0.000347	0.0186
0.0148	0.00246	8.27	0.0126	0.0173	0.000344	0.0186

						0.0187 ^b _± 0.0001

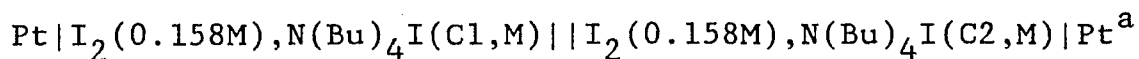
a. In 95% pyridine and 5% n-heptane.

b. In this cell, the concentration of I₂ was 0.159M

and 90% Py, rather than 90% Py, was present in both half-cells.

TABLE 28

EMF data on the cell



C1,M	C2,M	E,mv	Y1,M	Y2,M	K1,M ²	X,M
0.00557	0.00278	1.92	0.0159	0.0171	0.000342	0.0185
0.00802	0.00267	3.41	0.0163	0.0186	0.000396	0.0199
0.0103	0.00257	5.12	0.0146	0.0178	0.000363	0.0190
0.0124	0.00248	6.51	0.0139	0.0179	0.000365	0.0191
0.0143	0.00239	7.69	0.0135	0.0182	0.000374	0.0193

						0.0192 _± 0.0004

0.00571	0.00286	1.89	0.0165	0.0178	0.000368	0.0192
0.00823	0.00274	3.58	0.0158	0.0181	0.000378	0.0194
0.0105	0.00264	5.12	0.0148	0.0181	0.000375	0.0194
0.0127	0.00254	6.50	0.0143	0.0184	0.000384	0.0196
0.0147	0.00245	7.74	0.0137	0.0186	0.000390	0.0198

						0.0195 ^b _± 0.0002

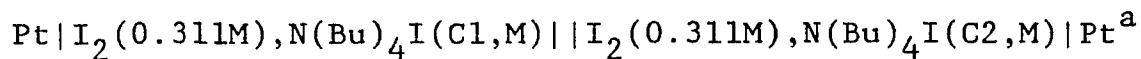
a. In 80% pyridine and 20% n-heptane.

b. In this cell, the concentration of I₂ was 0.159M

and 70% Py, rather than 80% Py, was present in both half-cells.

TABLE 29

EMF data on the cell



C1,M	C2,M	E,mv	Y1,M	Y2,M	K1,M ²	X,M
0.0107	0.00536	1.98	0.0294	0.0317	0.00118	0.0343
0.0154	0.00515	3.73	0.0279	0.0323	0.00121	0.0348
0.0198	0.00495	5.33	0.0266	0.0327	0.00123	0.0351
0.0238	0.00477	6.73	0.0255	0.0331	0.00125	0.0354
0.0276	0.00460	8.16	0.0239	0.0328	0.00123	0.0351

						0.0349 _± 0.0004

0.0111	0.00558	1.81	0.0337	0.0361	0.00151	0.0388
0.0161	0.00536	3.50	0.0317	0.0363	0.00151	0.0389
0.0206	0.00515	5.11	0.0292	0.0356	0.00145	0.0381
0.0248	0.00496	6.53	0.0277	0.0357	0.00145	0.0381
0.0287	0.00478	7.90	0.0260	0.0354	0.00142	0.0377

						0.0383 ^b _± 0.0005

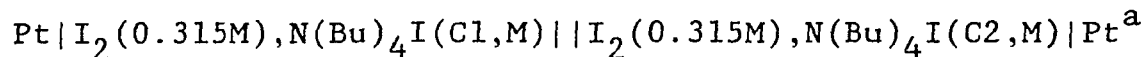
a. In 95% pyridine and 5% n-heptane.

b. In this cell, the concentration of I₂ was 0.314M

and 90% Py, rather than 95% Py, was present in both half-cells.

TABLE 30

EMF data on the cell



C1,M	C2,M	E,mv	Y1,M	Y2,M	K1,M ²	X,M
0.0111	0.00555	1.85	0.0331	0.0355	0.00146	0.0382
0.0160	0.00533	3.41	0.0325	0.0371	0.00158	0.0397
0.0205	0.00512	4.90	0.0307	0.0372	0.00157	0.0396
0.0247	0.00493	6.25	0.0293	0.0374	0.00158	0.0397
0.0285	0.00476	7.60	0.0273	0.0367	0.00152	0.0390

						0.0392 _± 0.0006

0.0114	0.00570	2.12	0.0289	0.0314	0.00117	0.0342
0.0164	0.00547	4.02	0.0271	0.0317	0.00118	0.0344
0.0210	0.00526	5.71	0.0257	0.0321	0.00120	0.0346
0.0253	0.00507	7.17	0.0248	0.0328	0.00124	0.0352
0.0293	0.00489	8.57	0.0236	0.0329	0.00125	0.0353

						0.0347 ^b _± 0.0005

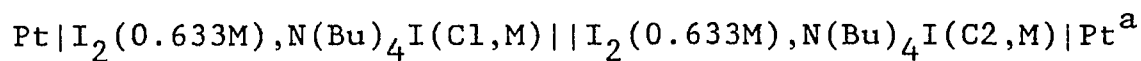
a. In 80% pyridine and 20% n-heptane.

b. In this cell, the concentration of I₂ was 0.311M

and 70% Py, rather than 80% Py, was present in both half-cells.

TABLE 31

EMF data on the cell



C1,M	C2,M	E,mv	Y1,M	Y2,M	K1,M ²	X,M
0.0216	0.0108	2.02	0.0580	0.0628	0.00462	0.0680
0.0311	0.0104	3.94	0.0527	0.0614	0.00441	0.0664
0.0399	0.00998	5.63	0.0498	0.0620	0.00446	0.0668
0.0481	0.00961	7.32	0.0458	0.0609	0.00430	0.0656
0.0556	0.00927	8.82	0.0429	0.0606	0.00423	0.0650

						0.0665 _± 0.0011

0.0222	0.0111	2.03	0.0593	0.0642	0.00483	0.0695
0.0320	0.0107	3.89	0.0551	0.0641	0.00480	0.0693
0.0411	0.0103	5.61	0.0515	0.0641	0.00476	0.0690
0.0494	0.00989	7.12	0.0489	0.0646	0.00481	0.0693
0.0572	0.00954	8.55	0.0462	0.0645	0.00478	0.0691

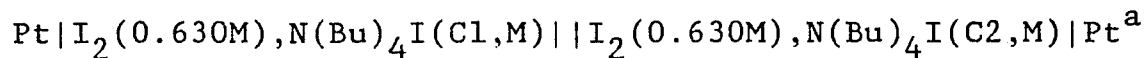
						0.0692 ^b _± 0.0001

a. In 95% pyridine and 5% n-heptane.

b. In this cell, the concentration of I₂ was 0.631M and 90% Py, rather than 95% Py, was present in both half-cells.

TABLE 32

EMF data on the cell



C1,M	C2,M	E,mv	Y1,M	Y2,M	K1,M ²	X,M
0.0224	0.0111	1.97	0.0626	0.0676	0.00533	0.0730
0.0322	0.0107	3.61	0.0611	0.0703	0.00569	0.0755
0.0413	0.0103	5.37	0.0549	0.0677	0.00528	0.0727
0.0497	0.00994	6.87	0.0517	0.0676	0.00525	0.0724
0.0575	0.00958	8.22	0.0492	0.0679	0.00526	0.0725

						0.0732 _± 0.0013

0.0227	0.0113	1.92	0.0651	0.0701	0.00571	0.0756
0.0326	0.0109	3.66	0.0606	0.0698	0.00564	0.0751
0.0418	0.0105	5.25	0.0571	0.07000	0.00564	0.0751
0.0504	0.0101	6.67	0.0546	0.06708	0.00573	0.0757
0.0583	0.00971	7.95	0.0524	0.06714	0.00580	0.0762

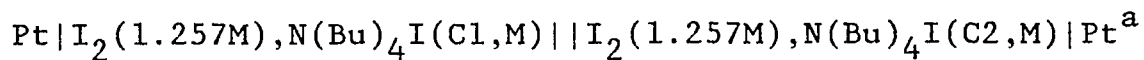
						0.0756 ^b _± 0.0004

a. In 80% pyridine and 20% n-heptane.

b. In this cell, the concentration of I₂ was 0.633M
and 70% Py, rather than 80% Py, was present in both half-cells.

TABLE 33

EMF data on the cell



C1,M	C2,M	E,mv	Y1,M	Y2,M	K1,M ²	X,M
0.0431	0.0215	2.01	0.1168	0.1264	0.0187	0.1367
0.0621	0.0207	3.80	0.1103	0.1279	0.0190	0.1379
0.0796	0.0199	5.52	0.1019	0.1265	0.0185	0.1360
0.0958	0.0192	7.05	0.0961	0.1265	0.0184	0.1358
0.1108	0.0185	8.59	0.0889	0.1243	0.0178	0.1334

						0.136 <u>±</u> 0.002

0.0446	0.0223	1.88	0.1303	0.1403	0.0228	0.1510
0.0642	0.0214	3.61	0.1216	0.1399	0.0226	0.1503
0.0823	0.0206	5.10	0.1169	0.1426	0.0233	0.1526
0.0990	0.0198	6.54	0.1103	0.1423	0.0231	0.1519
0.1146	0.0191	7.85	0.1048	0.1424	0.0230	0.1517

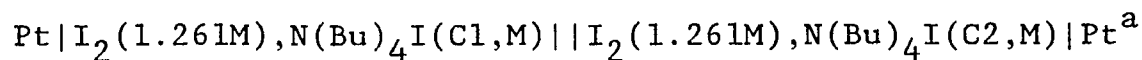
						0.152 ^b <u>±</u> 0.001

a. In 95% pyridine and 5% n-heptane.

b. In this cell, the concentration of I₂ was 1.259M
and 90% Py, rather than 95% Py, was present in both half-cells.

TABLE 34

EMF data on the cell



C1,M	C2,M	E,mv	Y1,M	Y2,M	K1,M ²	X,M
0.0445	0.0223	2.23	0.1061	0.1157	0.01598	0.1264
0.0641	0.0214	4.29	0.0975	0.1153	0.01577	0.1256
0.0822	0.0205	6.11	0.0919	0.1167	0.01601	0.1265
0.0989	0.0198	7.79	0.0861	0.1167	0.01593	0.1262
0.1145	0.0191	9.30	0.0816	0.1173	0.01600	0.1265

						0.126 <u>+</u> 0.001

0.0454	0.0227	1.93	0.1287	0.1387	0.0224	0.1497
0.0654	0.0218	3.69	0.1205	0.1391	0.0224	0.1496
0.0839	0.0209	5.25	0.1150	0.1411	0.0229	0.1512
0.1009	0.0202	6.73	0.1080	0.1404	0.0226	0.1502
0.1168	0.0195	8.27	0.0991	0.1368	0.0214	0.1463

						0.149 ^b <u>+</u> 0.002

a. In 80% pyridine and 20% n-heptane.

b. In this cell, the concentration of I₂ was 1.261M
and 70% Py, rather than 80% Py, was present in both half-cells.

Appendix C

Temperature effect on the EMF data

TABLE 35

Temperature effect on the EMF data on the cell
 $\text{Pt}|\text{I}_2(0.0422\text{M}),\text{NaI}(\text{C1},\text{M})||\text{I}_2(0.0422\text{M}),\text{NaI}(\text{C2},\text{M})|\text{Pt}^{\text{a}}$

Temp., °K	C1,M	C2,M	E,mv	X,M	K_{eq}
298	0.00172	0.000575	2.93	0.00497	0.0237
313	-----	-----	3.35	0.00456	0.0190
328	-----	-----	3.78	0.00423	0.0157
313	-----	-----	3.32	0.00504	0.0194
298	-----	-----	2.89	0.00504	0.0246
298	0.00266	0.000532	5.37	0.00501	0.0242
313	-----	-----	6.07	0.00464	0.0198
328	-----	-----	6.89	0.00427	0.0161
313	-----	-----	6.03	0.00467	0.0202
298	-----	-----	5.42	0.00496	0.0236

a. In pure pyridine.

TABLE 36

Temperature effect on the EMF data on the cell
 $\text{Pt} | \text{I}_2(0.0778\text{M}), \text{NaI}(C_1, \text{M}) || \text{I}_2(0.0778\text{M}), \text{NaI}(C_2, \text{M}) | \text{Pt}^a$

Temp., °K	C ₁ , M	C ₂ , M	E, mv	X, M	K _{eq}
298	0.00423	0.00141	3.89	0.00917	0.0238
313	-----	-----	4.46	0.00838	0.0188
328	-----	-----	4.97	0.00787	0.0161
313	-----	-----	4.43	0.00844	0.0192
298	-----	-----	3.93	0.00907	0.0231
298	0.00653	0.00131	7.02	0.00930	0.0247
313	-----	-----	7.91	0.00863	0.0203
328	-----	-----	9.02	0.00789	0.0162
313	-----	-----	7.90	0.00865	0.0204
298	-----	-----	7.05	0.00925	0.0243

a. In pure pyridine.

TABLE 37

Temperature effect on the EMF data on the cell
 $\text{Pt} | \text{I}_2(0.157\text{M}), \text{NaI}(C1, \text{M}) || \text{I}_2(0.157\text{M}), \text{NaI}(C2, \text{M}) | \text{Pt}^a$

Temp., °K	C1, M	C2, M	E, mv	X, M	K_{eq}
298	0.00825	0.00275	3.81	0.0183	0.0231
313	-----	-----	4.35	0.0168	0.0185
328	-----	-----	4.98	0.0153	0.0146
313	-----	-----	4.36	0.0167	0.0183
298	-----	-----	3.82	0.0182	0.0228
298	0.0127	0.00254	7.05	0.0180	0.0221
313	-----	-----	8.02	0.0166	0.0180
328	-----	-----	8.91	0.0157	0.0156
313	-----	-----	8.00	0.0166	0.0180
298	-----	-----	7.06	0.0180	0.0221

a. In pure pyridine.

TABLE 38

Temperature effect on the EMF data on the cell
 $\text{Pt}|\text{I}_2(0.628\text{M}),\text{NaI}(\text{C1},\text{M})||\text{I}_2(0.628\text{M}),\text{NaI}(\text{C2},\text{M})|\text{Pt}^{\text{a}}$

Temp., °K	C1,M	C2,M	E,mv	X,M	K_{eq}
298	0.0322	0.0107	3.69	0.0738	0.0236
313	-----	-----	4.25	0.0671	0.0184
328	-----	-----	4.79	0.0623	0.0153
313	-----	-----	4.27	0.0668	0.0182
298	-----	-----	3.68	0.0740	0.0238
298	0.0495	0.00991	6.71	0.0739	0.0237
313	-----	-----	7.52	0.0691	0.0199
328	-----	-----	8.31	0.0653	0.0172
313	-----	-----	7.51	0.0692	0.0199
298	-----	-----	6.70	0.0740	0.0238

a. In pure pyridine.

TABLE 39

Temperature effect on the EMF data on the cell
 $\text{Pt}|\text{I}_2(1.265\text{M}),\text{NaI}(\text{C1},\text{M})||\text{I}_2(1.265\text{M}),\text{NaI}(\text{C2},\text{M})|\text{Pt}^{\text{a}}$

Temp., °K	C1,M	C2,M	E,mv	X,M	K_{eq}
298	0.0639	0.0213	3.50	0.154	0.0259
313	-----	-----	4.03	0.141	0.0206
328	-----	-----	4.63	0.128	0.0161
313	-----	-----	4.05	0.140	0.0202
298	-----	-----	3.51	0.154	0.0259
298	0.0987	0.0197	6.58	0.150	0.0242
313	-----	-----	7.72	0.134	0.0181
328	-----	-----	8.51	0.127	0.0158
313	-----	-----	7.74	0.134	0.0181
298	-----	-----	6.60	0.150	0.0242

a. In pure pyridine.

REFERENCES

1. Audrieth, L.F.; Birr, E.J. J. Am. Chem. Soc. 1933, 55, 668.
2. Hartley, K.; Skinner, H.A. Trans. Faraday Soc. 1950, 26, 621.
3. Reid, C.; Mulliken, R.S. J. Am. Chem. Soc. 1954, 76, 3869
4. Mckinney, W.J.; Popov, A.I. J. Am. Chem. Soc. 1969, 91, 5215.
5. Kortum, G.; Wilski, H. Z. Physik. Chem. 1953, 202, 35.
6. Zingaro, R.; Vander-Werf, C.A.; Kleinberg, J. J. Am. Chem. Soc. 1951, 73, 88.
7. Pezzatini, G.; Guidelli, R. Electrochim. Acta 1971, 16, 1415.
8. Nigretto, J.M.; Josefowicz, M. Electrochim. Acta 1974, 19, 809.
9. Nigretto, J.M.; Josefowicz, M. "Pyridine as a Nonaqueous Solvent" in Lagowski, J.J. Ed.; "The Chemistry of Nonaqueous Solvents" Academic Press: 1978, Chapter 5.
10. Mulliken, R.S. J. Am. Chem. Soc. 1952, 74, 811.
11. Aronson, S; Epstein, P; Aronson, D.B.; Wieder, G. J. Phys. Chem. 1982, 86, 1035.
12. French, C.M.; Muggleton, D.E. J. Chem. Soc. 1957, 2131.
13. Kauffman, G.B.; Stevens, K.L. "Monopyridineiodine(I) Chloride" in Kleinberg, J.; Ed.; "Inorganic Synthesis" Vol. VII; McGraw Hill: 1963.
14. Carlsohn, H. "Über Eine Neue Klasse von Verbindungen des Positiv Einwertigen Jods" Verlag Hirzel: Leipzig 1932.

15. Awtrey, A.D.; Connick, R.E. J. Am. Chem. Soc. 1951, 73, 1842.
16. Vedel, J.; Tremillon, B. J. Electroanal. Chem. 1960, 1, 241.
17. Cizak, A.; Elving, P.J. J. Electrochem. Soc. 1963, 110, 160.
18. Kolthoff, I.M.; Coetze, J.F. J. Am. Chem. Soc. 1957, 79, 1852.
19. Popov, A.I.; Geske, D.H. J. Am. Chem. Soc. 1958, 80, 1340.
20. Nelson, I.V.; Iwamoto, R.T. J. Electroanal. Chem. 1964, 7, 218.
21. Plichon, V.; Badoz-Lambling, J.; Charlot, G. Bull. Soc. Chim. Fr. 1964, 287.
22. Piccardi, G.; Guidelli, R. J. Phys. Chem. 1967, 71, 3020.
23. Dryhurst, G.; Elving, J. Anal. Chem. 1967, 39, 606.
24. Iwamoto, R.T. Anal. Chem. 1959, 31, 955.
25. Bocarsly, A.B.; Sinha, S. J. Electroanal. Chem. 1982, 140, 167.
26. Mulliken, R.S.; Person, W.B. "Molecular Complexes" John Wiley and Sons: N.Y. 1969.
27. Tamres, M.; Yarwood, J. "Complexes of N and π Donors with Hologens and Related σ Acceptors" in Yarwood, J.; Ed.; "Spectroscopy and Structure of Molecular Complexes" Plenum press: London, 1973, Chapter 3.
28. Kaya, K.; Mikami, N.; Uoagawa, Y.; Ito, M. Chemical Physics Letters 1972, 16, 151.
29. Kiefer, W.; Bernstein, H.J. Chemical Physics Letters 1972, 16, 5.
30. Klaboe, P. J. Am. Chem. Soc. 1967, 89, 3667.
31. Kleinberg, J.; Colton, E.; Sattizahn, J.; Vanderwerf, C.A. J. Am. Chem. Soc. 1953, 75, 442.
32. Toyoda, K.; Person, W.B. J. Am. Chem. Soc. 1966, 88, 1629.

33. Dewar, M.J.S.; Thompson, C.C. Tetrahedron Suppl. 1966, 7, 97.
34. Wantig, P. Z. Physik. Chem. 1909, 68, 513.
35. Charlsohn, H. Z. Angew. Chem. 1933, 46, 747.
36. Buckles, R.E.; Yuk, J.p.; Popov, A.I. J. Am. Chem. Soc. 1952, 74, 4379.
37. Larson, R.C.; Iwamoto, R.T.; Adams, R.N. Anal. Chim. Acta. 1961, 25, 371.
38. Kleinberg, J.; Davidson, A.W. Chem. Revs. 1948, 42, 601.